

AperTO - Archivio Istituzionale Open Access dell'Università di Torino

Transport properties and Langevin dynamics of heavy quarks and quarkonia in the Quark Gluon Plasma

This is the author's manuscript

Original Citation:

Availability:

This version is available <http://hdl.handle.net/2318/133382> since

Terms of use:

Open Access

Anyone can freely access the full text of works made available as "Open Access". Works made available under a Creative Commons license can be used according to the terms and conditions of said license. Use of all other works requires consent of the right holder (author or publisher) if not exempted from copyright protection by the applicable law.

(Article begins on next page)

Transport properties and Langevin dynamics of heavy quarks and quarkonia in the Quark Gluon Plasma

A. Beraudo^{a,b}, A. De Pace^b, W.M. Alberico^{a,b}, A. Molinari^{a,b}

^a*Dipartimento di Fisica Teorica dell'Università di Torino,
via P.Giuria 1, I-10125 Torino, Italy*

^b*Istituto Nazionale di Fisica Nucleare, Sezione di Torino,
via P.Giuria 1, I-10125 Torino, Italy*

Abstract

Quark Gluon Plasma transport coefficients for heavy quarks and $Q\bar{Q}$ pairs are computed through an extension of the results obtained for a hot QED plasma by describing the heavy-quark propagation in the eikonal approximation and by weighting the gauge field configurations with the Hard Thermal Loop effective action. It is shown that such a model allows to correctly reproduce, at leading logarithmic accuracy, the results obtained by other independent approaches. The results are then inserted into a relativistic Langevin equation allowing to follow the evolution of the heavy-quark momentum spectra. Our numerical findings are also compared with the ones obtained in a strongly-coupled scenario, namely with the transport coefficients predicted (though with some limitations and ambiguities) by the AdS/CFT correspondence.

Key words: Quark Gluon Plasma, heavy quarks, transport, Hard Thermal Loop, Langevin equation

PACS: 11.10.Wx, 12.38.Mh, 14.65.Dw, 14.65.Fy, 21.65.Qr, 25.75.Cj, 25.75.Nq

1. Introduction

Ultra-relativistic heavy-ion experiments at the Relativistic Heavy Ion Collider (RHIC) and (in the near future) at the Large Hadron Collider (LHC) aim at reproducing, in a small region of space-time, the conditions of the primordial universe, with such a large energy-density to allow the onset of the deconfined phase of QCD. Through high-energy nucleus-nucleus collisions one should be able to explore the QCD phase-diagram in the region of high temperature and (almost) vanishing baryon density.

However the fireball of quarks and gluons possibly produced in such collisions expands and cools, so that the only strongly-interacting particles reaching the detectors are again color-singlet hadrons. Hence the need to extract information on what occurred before hadronization: whether a thermalized Quark Gluon Plasma (QGP) was produced and, if so, which are its properties.

Heavy quarks (charm and bottom) and quarkonia are well suited for this purpose. Due to their large mass they are produced in the very early stages of the collision and, before giving rise to experimentally detectable signals from their decays into hadrons and/or leptons, they have to cross the hot (possibly) deconfined region. By comparing

the data collected in nucleus-nucleus collisions with the ones coming from benchmark experiments, like proton-proton or proton-nucleus collisions, in which one does not expect QGP formation, one eventually can prove the formation of a totally new kind of medium. In particular, a lot of interest on quarkonia was triggered by the seminal paper by Matsui and Satz [1] proposing the anomalous suppression of the J/Ψ in nucleus-nucleus collisions as an unambiguous signature of deconfinement.

For what concerns heavy quarks — giving rise to D and B mesons at hadronization — they can provide useful insight into the transport properties of the medium they cross. Due to their large mass they require a much longer time (by a factor M/T) than the light particles to thermalize; naively one expects that in an expanding medium with a quite short life-time (of order of $5 - 10$ fm/c) they can hardly approach thermal equilibrium. If, on the other hand, one found them to follow the flow of the fluid, this would be a signal of large friction and momentum-diffusion coefficients, whose origin would need an explanation.

RHIC data led to a description of the matter produced in the Au-Au collisions as a strongly-coupled QGP (sQGP). In particular the radial [2, 3] and elliptic (in semi-central collisions) flow [4, 5] observed in the p_T -spectra of detected hadrons suggested a picture of the QGP in the regime of temperatures accessible at RHIC more similar to a fluid (hence with very small mean-free-paths) — with a collective expansion driven by pressure gradients — than to a weakly-interacting gas of quarks and gluons. Furthermore, the strong suppression (by a factor of 5) of high- p_T hadrons [6, 7] with respects to elementary proton-proton collisions suggests that the QGP produced at RHIC is a very opaque medium.

Heavy quarks at RHIC are studied through the electrons arising from the semi-leptonic decays of D and B mesons. This makes it hard to draw definite conclusions on their flow and energy loss, due in particular to the difficulty of disentangling the charm and bottom contributions. However, recent measurements performed by the PHENIX [8] and STAR [9] collaborations seem to support a scenario with the charm quark following the flow of the medium and experiencing a strong energy loss, comparable to the one seen in light hadron spectra. Different explanations were advocated to account for such an apparently rapid thermalization, like the existence of resonant $Q\bar{q}$ states [10] above T_c or values of transport coefficients close to the bounds predicted by the AdS/CFT correspondence [11, 12, 13, 14, 15, 16], claimed to represent a good description of the sQGP for temperatures nearby T_c . See also Refs. [17, 18, 19, 20] for other approaches.

At LHC on the other hand one expects to produce a fireball with a larger initial temperature (possibly $T_0 \sim 800$ MeV) and a longer life-time. This could make weak-coupling calculations better justified. From the experimental side [21], the possibility of reconstructing also hadronic decays, like $D^0 \rightarrow K^- \pi^+$, in Pb-Pb collisions will remove the ambiguities encountered at RHIC.

Two are the main issues addressed in this paper, both related to the transport properties of charm and bottom quarks in a hot plasma. We first focus on the calculation of the transverse $\kappa_T(p)$ and longitudinal $\kappa_L(p)$ momentum-diffusion coefficients. We then make use of the above results to follow the approach of heavy quarks to thermal equilibrium through a numerical Langevin simulation. We confine ourselves to the case of a static medium, for temperatures spanning a range of experimental interest for LHC.

In order to calculate the coefficients $\kappa_T(p)$ and $\kappa_L(p)$ we perform a generalization to the QCD case of an approach developed in [22, 23] to describe heavy (static) “quarks” in

a hot plasma of electrons, positrons and photons. The latter represented in fact a system sharing important features with the QGP, but for which the possibility of employing in the calculations a Hard Thermal Loop (HTL) gaussian effective action allowed to study in an easy way important medium effects. This approach makes it possible to calculate also transport coefficients of $Q\bar{Q}$ pairs. This is important, since measurements of p_T spectra of quarkonia may allow to discriminate different scenarios. One expects in fact that the measured J/ψ 's in the final state should tend to follow the flow of the fireball, if they came from the recombination of charm quarks free of floating around in the plasma phase. On the contrary, if they remained bound and sufficiently close in space also in the deconfined environment, they would suffer less collisions in the colored medium, as they would be seen mostly as a neutral object.

As already mentioned, we then insert the above transport coefficients into a relativistic Langevin equation, allowing to follow the stochastic momentum evolution of the heavy quarks in the QGP. Their initial momentum p_0 is taken of the order of the average transverse momentum \bar{p}_T of c and b quarks produced in nucleus-nucleus collisions at RHIC and LHC. The latter can be, for instance, evaluated from a sample of events generated by PYTHIA [24] with a proper tuning of the parameters.

Dealing with the relativistic Langevin equation, with a momentum dependent diffusion term, is a non-trivial task. Actually, the latter belongs to the class of stochastic differential equations, which represents an open field of mathematical research, and requires a careful discretization procedure. In particular, the drag coefficient has to be appropriately tuned in order to lead, in the continuum limit, to a Fokker-Planck equation admitting the relativistic Maxwell distribution as a stationary solution. We devote Appendix B to discuss these issues in detail.

Our paper is organized as follows. In Sec. 2 we summarize well known results on the diffusion of non-relativistic heavy quarks in a hot plasma, displaying how the Langevin equation can be used as an effective theory to deal with the problem. However, in high-energy collisions charm and bottom spectra, though rapidly decreasing, have long power-law tails extending up to very large transverse momenta. Hence the need of extending the Langevin equation to the relativistic case. In Sec. 3 we thus present the calculation of the transport coefficients for a quark with a generic momentum p . In Sec. 4 the approach is extended to deal with a $Q\bar{Q}$ pair. Sec. 5 is devoted to the numerical results both for the transport coefficients and for the Langevin evolution of heavy-quark spectra. Finally, in Sec. 6 we discuss our results and draw our conclusions. Some technical details are given in the appendices. In Appendix A we recall the essential formulas for the HTL gluon propagators and spectral functions which are employed in the text. In Appendix B we give a self-contained discussion of the problems one has to face in solving the relativistic Langevin equation. In Appendix C we report the results of the kinetic calculation of the momentum-diffusion coefficient in the non-relativistic case, which is used as a benchmark to have some control on the uncertainties related to our effective HTL approach.

2. Langevin approach for heavy quarks in the QGP: a brief summary

The Langevin equation has been recently employed by several authors [25, 26, 27, 28, 29, 30] as an effective theory to describe the evolution in coordinate and momentum space of heavy quarks in a hot plasma. In this section we briefly summarize the main aspects of such an approach, focusing in particular on its range of validity and on the

information on the medium properties that can be extracted from the study of the heavy quark propagation.

For the sake of simplicity our introductory discussion refers to the non-relativistic case, i.e. with the heavy quarks not too far from thermal equilibrium. This will be sufficient for the above purposes. Actually, in heavy-ion collisions, c and b quarks are produced with a sizable transverse momentum, so that a relativistic study is in order. This however would introduce some technicalities; hence we postpone it to the following sections, where we shall see that, as long as $T/E \ll 1$, the Langevin approach remains justified.

In [22, 31] it was shown that the interaction rate of a very massive (i.e. with $M \gg T$) quark at rest in a hot plasma is of order g^2T and is given by (here we consider the QED case):

$$\Gamma = g^2T \int \frac{d\mathbf{q}}{(2\pi)^3} \frac{\pi m_D^2}{(\mathbf{q}^2 + m_D^2)^2 q} = \frac{g^2T}{4\pi}. \quad (1)$$

Since the Debye mass $m_D \sim gT$ is the only scale within the integral, the typical momentum exchanged in the interaction will be of its order ¹. In particular the maximum of the integrand occurs at $\bar{q} = m_D/\sqrt{3}$, so that most of the kicks received by the heavy quark will involve the exchange of soft electrostatic photons (since M is very large, one can neglect magnetic interactions and consider the static limit) with momentum, and virtuality, $q \sim gT$. Hence the duration of a collision $\tau_{\text{coll}} \sim 1/gT$ will be well separated, at least in the weak coupling regime, from the average time interval between two scattering events $\Delta\tau \equiv 1/\Gamma \sim 1/g^2T$. Since $\tau_{\text{coll}} \ll \Delta\tau$, one is then allowed to treat the diffusion of the heavy quarks as resulting from the sum of many uncorrelated momentum kicks.

Due to the large mass M , a huge number of collisions is required for an ensemble of heavy quarks to thermalize. At thermal equilibrium, from the equipartition theorem, one has $\bar{p}_{\text{heavy}} = \sqrt{3MT}$, while for the light particles $\bar{p}_{\text{light}} \sim T$, hence

$$\langle p_{\text{heavy}}^2 \rangle \sim \frac{M}{T} \langle p_{\text{light}}^2 \rangle, \quad (2)$$

the same relation expressing the number of random collisions required to change the average squared-momentum by a factor of order one. In the case $M \gg T$ the heavy-quark relaxation time will then be much larger than the one for the light particles of the medium, namely:

$$\tau_{\text{heavy}} \sim \frac{M}{T} \tau_{\text{light}} \underset{g \ll 1}{\sim} \frac{M}{T} \frac{1}{g^4 T \ln(1/g)}, \quad (3)$$

where the last estimate refers to the weak-coupling regime (τ_{light} being of the order of the time interval between two hard collisions) and will be shown to hold in the following.

In the Langevin approach [32] the equation of motion for a non-relativistic heavy quark reads

$$\frac{dp^i}{dt} = -\eta_D p^i + \xi^i(t), \quad (4)$$

¹Note that the total interaction rate is independent on the value of m_D , which is only relevant to set the typical scale of exchanged momenta and to prevent infrared divergences by screening the interaction.

where the right hand side is given by the sum of a friction force (described by the *drag* coefficient η_D) and a noise term, which is fixed by its temporal correlator:

$$\langle \xi^i(t) \xi^j(t') \rangle = \kappa \delta^{ij} \delta(t - t'). \quad (5)$$

The noise arises from the random uncorrelated momentum kicks received from the medium. Eq. (4) can be solved by discretizing the time derivative with a time-step Δt sufficiently large to include many collisions, but much shorter than the relaxation time of the heavy quark. The latter represents the typical time-scale over which one would like to follow the momentum evolution. The condition to be fulfilled is then:

$$\tau_{\text{light}} \ll \Delta t \ll \tau_{\text{heavy}} \sim \frac{M}{T} \tau_{\text{light}}. \quad (6)$$

The *momentum diffusion coefficient* κ represents the *averaged squared momentum* acquired by the heavy quark per unit time,

$$\kappa \equiv \frac{1}{3} \left\langle \frac{\Delta \mathbf{p}^2}{\Delta t} \right\rangle, \quad (7)$$

and arises from the cumulated effect of many kicks suffered in the elementary time-step. It can be calculated from Eq. (1), by weighting the differential interaction rate with the squared momentum transfer, thus getting

$$\begin{aligned} \kappa &= \frac{g^2 m_D^2 T}{6\pi} \int_0^{q_{\text{max}}} \frac{q^3 dq}{(q^2 + m_D^2)^2} \\ &= \frac{g^2 m_D^2 T}{12\pi} \left[\ln \frac{q_{\text{max}}^2 + m_D^2}{m_D^2} - \frac{q_{\text{max}}^2}{q_{\text{max}}^2 + m_D^2} \right]. \end{aligned} \quad (8)$$

Notice that, while the interaction rate is free of ultraviolet divergences — hard scatterings not occurring very frequently — in the calculation of transport coefficients the latter play a major role, since, in spite of being quite rare, they can lead to a sizable momentum transfer. In the above $q_{\text{max}} \sim T$ reflects an estimate of the maximum momentum exchange with a typical thermal particle. One often considers the result at Leading Logarithmic Accuracy (LLA):

$$\kappa_{\text{LLA}} = \frac{g^2 m_D^2 T}{6\pi} \int_{m_D}^{q_{\text{max}}} \frac{dq}{q} = \frac{g^2 m_D^2 T}{6\pi} \ln \frac{q_{\text{max}}}{m_D}, \quad (9)$$

where the argument of the logarithm is of order $1/g$, its precise numerical value representing the theoretical uncertainty of the present approach.

By requiring the momentum distribution to reach thermal equilibrium one gets the Einstein relation between the drag and momentum diffusion coefficients:

$$\eta_D = \frac{\kappa}{2MT}. \quad (10)$$

Concerning the evolution in space, from

$$\langle x^2(t) \rangle \underset{t \rightarrow \infty}{\sim} 6Dt, \quad \text{with} \quad x^i(t) = \int_0^t dt' \frac{p^i(t')}{M}, \quad (11)$$

one derives the (spatial) *heavy-quark diffusion coefficient*

$$D = \frac{T}{M\eta_D} = \frac{2T^2}{\kappa}, \quad (12)$$

whose expression at LLA follows from Eq. (9)

$$D^{\text{LLA}} = \frac{12\pi T}{g^2 m_D^2 \ln \frac{q_{\text{max}}}{m_D}}. \quad (13)$$

For the heavy-quark relaxation time one has then:

$$\tau_{\text{heavy}} \equiv \frac{1}{\eta_D} = \frac{M}{T} D. \quad (14)$$

By comparing Eqs. (3) and (14) one gets the interesting result [26]

$$D \sim \tau_{\text{light}} \underset{g \ll 1}{\sim} \frac{1}{g^4 T \ln(1/g)}, \quad (15)$$

showing that the heavy quark diffusion coefficient gives a reasonable estimate of the relaxation time of the medium. We also notice that, in the weak coupling regime, from Eq. (13), one has $\tau_{\text{light}} \sim 1/g^4 T \ln(1/g)$.

For a recent study of the possibility of estimating heavy-quark transport coefficients from euclidean lattice simulations see Ref. [33].

3. Propagation of a heavy quark in a hot plasma: transport properties

We start our investigation by considering the propagation of a heavy quark in a hot ultra-relativistic plasma. When the quark is very massive and/or is endowed with a very large momentum $p \gg T$, it is reasonable to describe it within the eikonal approximation, in which it moves along a straight-line trajectory, acquiring a phase due to the interaction with the background gauge field.

One could argue that, due to the multiple kicks received from the particles of the medium, during its propagation the heavy quark would loose energy and acquire more and more transverse momentum, so that at some point the assumption of straight-line propagation should cease to be valid. However, one can take advantage of the huge separation, occurring for $E_p \gg T$, between the relaxation time of the medium, τ_{light} , and the much larger time required by the heavy quark to approach equilibrium. In order to evaluate transport coefficients (related for instance to heavy-quark energy loss, diffusion and momentum broadening), it is sufficient to follow the propagation of the quark for a time large compared to τ_{light} but still much shorter than the relaxation time of the high-momentum heavy quark. For this purpose our eikonal approach should be justified and indeed turns out to provide results in agreement (at least at Leading Logarithmic Accuracy) with the ones obtained in other approaches as, for example, by solving the Maxwell equations in a dielectric medium [34, 35, 36]. If one is really interested in following the relaxation of the heavy quarks toward thermal equilibrium, then one can use the above findings for the transport coefficients and insert them into the Langevin or Fokker-Planck equations.

Following the approach developed in Refs.[22, 23], the configurations of the gauge-field entering into the eikonal phase are weighted by the HTL effective action. We start from the QED case (i.e. a plasma of photons, electrons and positrons), in which the latter is gaussian; this allows to perform the functional integral exactly, leading to an exact exponentiation of the gauge-field propagator. Later we will show how the results for the transport properties can be generalized to the QCD case, yet recovering well known findings.

In analogy with the approach adopted in Refs. [22, 37], we consider the retarded propagator of a heavy quark — which is treated as a test particle — created at $(0, \mathbf{r}'_1)$ and annihilated at (t, \mathbf{r}_1) ; it is defined as

$$G^R(t, \mathbf{r}_1 | 0, \mathbf{r}'_1) \equiv i \theta(t) \langle \psi(t, \mathbf{r}_1) \psi^\dagger(0, \mathbf{r}'_1) \rangle, \quad (16)$$

where the expectation value refers to a thermal average over the states of a hot medium of light particles. In the eikonal approximation it is given by:

$$G^R(t, \mathbf{r}_1 | 0, \mathbf{r}'_1) = i \theta(t) \delta(\mathbf{r}_1 - \mathbf{r}'_1 - \mathbf{v}t) \overline{G}(t). \quad (17)$$

In the above, the eikonal phase (which is complex, the imaginary part accounting for the effects of collisions) is expressed in terms of the *real-time* gauge-field propagator given in Appendix A:

$$\overline{G}(t) = \exp \left[\frac{i}{2} \int d^4x \int d^4y J^\mu(x) D_{\mu\nu}(x-y) J^\nu(y) \right], \quad (18)$$

where the current describing the propagation of the heavy quark is given by:

$$J^\mu(x) = g \theta(x^0) \theta(t - x^0) \delta(\mathbf{x} - \mathbf{r}'_1 - \mathbf{v}x^0) (1, \mathbf{v}). \quad (19)$$

After expressing the gauge propagator in Fourier space one gets:

$$\overline{G}(t) = \exp \left\{ \frac{i}{2} g^2 \int \frac{d\omega}{2\pi} \int \frac{d\mathbf{q}}{(2\pi)^3} \frac{2 [1 - \cos(\omega - \mathbf{q} \cdot \mathbf{v})t]}{(\omega - \mathbf{q} \cdot \mathbf{v})^2} \times [D_L(\omega, q) + v^2 (1 - (\hat{\mathbf{v}} \cdot \hat{\mathbf{q}})^2) D_T(\omega, q)] \right\}, \quad (20)$$

whose large-time behavior can be obtained from the limit

$$\lim_{t \rightarrow \infty} \frac{1 - \cos(\omega - \mathbf{q} \cdot \mathbf{v})t}{(\omega - \mathbf{q} \cdot \mathbf{v})^2} = \pi t \delta(\omega - \mathbf{q} \cdot \mathbf{v}). \quad (21)$$

In particular the probability of finding the heavy quark with momentum $\mathbf{p} = \gamma M \mathbf{v}$ will tend to decrease due to the collisions with the plasma particles, whose effects are encoded into the imaginary part of the HTL gauge-field propagator (see Appendix A):

$$\text{Im } D_{L/T}(\omega, q) = \rho_{L/T}(\omega, q) \left(N(\omega) + \frac{1}{2} \right). \quad (22)$$

This allows to *formally* define an interaction rate for a quark propagating with velocity \mathbf{v} (taken in the following along the z -axis), which turns out to be given by (the spectral

functions being odd)

$$\begin{aligned}\Gamma &= g^2 \int d\omega \int \frac{d\mathbf{q}}{(2\pi)^3} \delta(\omega - \mathbf{q} \cdot \mathbf{v}) [\rho_L(\omega, q) + v^2 (1 - (\hat{\mathbf{v}} \cdot \hat{\mathbf{q}})^2) \rho_T(\omega, q)] N(\omega) \\ &\equiv g^2 \int d\omega \int \frac{d\mathbf{q}}{(2\pi)^3} \delta(\omega - \mathbf{q} \cdot \mathbf{v}) \tilde{\rho}(\omega, \mathbf{q}) N(\omega).\end{aligned}\quad (23)$$

Note that, strictly speaking, the above expression develops an infrared divergence arising from the exchange of long-wavelength magneto-static gluons². However the above processes cannot affect the transport properties related to the heavy-quark propagation (energy loss, momentum broadening, ...), since they are related to negligible energy/momentum exchanges. Hence we can take advantage of Eq. (23) for the computation of the transport coefficients we are interested in.

The energy loss per unit length is then given by:

$$\frac{dE}{dx} = \frac{g^2}{v} \int d\omega \int \frac{d\mathbf{q}}{(2\pi)^3} \delta(\omega - \mathbf{q} \cdot \mathbf{v}) \tilde{\rho}(\omega, \mathbf{q}) \omega N(\omega).\quad (24)$$

The Dirac delta

$$\delta(\omega - \mathbf{q} \cdot \mathbf{v}) = \frac{1}{qv} \delta\left(\cos\theta - \frac{\omega}{qv}\right)\quad (25)$$

can be exploited to perform the angular integration. Furthermore, since the spectral function is odd, one can replace the Bose distribution with its even part

$$N(\omega) \rightarrow \frac{N(\omega) + N(-\omega)}{2} = -\frac{1}{2},\quad (26)$$

thus obtaining

$$\begin{aligned}-\frac{dE}{dx} &= \frac{g^2}{4\pi^2 v^2} \int_0^{q_{\max}} dq q \int_0^{vq} d\omega \omega \left[\rho_L(\omega, q) + \left(v^2 - \frac{\omega^2}{q^2}\right) \rho_T(\omega, q) \right] \\ &\equiv \frac{g^2}{4\pi^2 v^2} \int_0^{q_{\max}} dq q \int_0^{vq} d\omega \omega \bar{\rho}(\omega, q),\end{aligned}\quad (27)$$

where, in the high-energy limit, $q_{\max} \sim \sqrt{ET}$, with E the energy of the heavy quark, is the maximum momentum transfer in a collision with a plasma particle, whose typical momentum is of order T . At LLA the energy loss can be computed analytically, by setting a lower bound of order m_D in the momentum integration and using for the spectral functions the expressions given in Eq. (76). One gets:

$$\begin{aligned}-\frac{dE}{dx}\Big|_{\text{LLA}} &= \frac{g^2 m_D^2}{4\pi v^2} \int_{m_D}^{q_{\max}} \frac{dq}{q^4} \int_0^{vq} d\omega \omega^2 \left[1 + \frac{v^2 - \omega^2/q^2}{2(1 - \omega^2/q^2)} \right] \\ &= \frac{g^2 m_D^2}{4\pi v^2} \int_{m_D}^{q_{\max}} \frac{dq}{q} \int_0^v dx x^2 \left[1 + \frac{v^2 - x^2}{2(1 - x^2)} \right].\end{aligned}\quad (28)$$

²Actually, lattice QCD results provide evidence for the existence of a non vanishing *magnetic mass* [38], of non-perturbative origin, which would eliminate the above divergence. This in principle could affect our results for the transport coefficients, but such an issue lies beyond the scopes of the present paper.

After performing the integrals one gets:

$$-\frac{dE}{dx}\Big|_{\text{LLA}} = \frac{g^2 m_D^2}{8\pi v} \ln \frac{q_{\text{max}}}{m_D} \left[1 - \frac{1-v^2}{2v} \ln \frac{1+v}{1-v} \right], \quad (29)$$

to be compared with the analogous result displayed in Eq. (B31) of Ref. [26] for the QCD case and quoting previous findings obtained in Refs. [39, 40].

We now address the calculation of the momentum diffusion coefficients κ_T and κ_L which will enter the noise term in the Langevin equation [see Eqs. (101) and (102)].

Let us start with the transverse momentum diffusion coefficient, representing the mean squared transverse momentum acquired per unit time by the heavy quark crossing the medium, namely:

$$\kappa_T \equiv \frac{1}{2} \langle \frac{\Delta p_T^2}{\Delta t} \rangle. \quad (30)$$

Also the latter can be computed starting from Eq. (23):

$$\kappa_T = \frac{g^2}{2} \int d\omega \int \frac{d\mathbf{q}}{(2\pi)^3} \delta(\omega - \mathbf{q} \cdot \mathbf{v}) \bar{\rho}(\omega, \mathbf{q}) q^2 (1 - \cos^2 \theta) N(\omega). \quad (31)$$

In the above only the odd part of the Bose distribution contributes to the integral, so that one can make the replacement

$$N(\omega) \rightarrow \frac{N(\omega) - N(-\omega)}{2} = \frac{1}{2} \coth \frac{\beta\omega}{2}, \quad (32)$$

thus obtaining:

$$\kappa_T = \frac{g^2}{8\pi^2 v} \int_0^{q_{\text{max}}} dq q \int_0^{vq} d\omega \bar{\rho}(\omega, q) q^2 \left(1 - \frac{\omega^2}{q^2 v^2} \right) \coth \frac{\beta\omega}{2}. \quad (33)$$

In analogy with the energy loss calculation, the LLA result for the transverse momentum diffusion is obtained by employing the corresponding approximate expression for the HTL spectral functions given in Appendix A, setting an infrared cutoff of order m_D in the momentum integration and assuming that the relevant contribution to the above expression is given by processes with small energy transfer, so that one can approximate

$$\coth \frac{\beta\omega}{2} \sim \frac{2T}{\omega}. \quad (34)$$

One obtains:

$$\begin{aligned} \kappa_T^{\text{LLA}} &= \frac{g^2 m_D^2}{8\pi v} \int_{m_D}^{q_{\text{max}}} \frac{dq}{q^2} \int_0^{vq} d\omega \omega \left[1 + \frac{v^2 - \omega^2/q^2}{2(1 - \omega^2/q^2)} \right] \left(1 - \frac{\omega^2}{q^2 v^2} \right) \frac{2T}{\omega} \\ &= \frac{g^2 T m_D^2}{4\pi v} \int_{m_D}^{q_{\text{max}}} \frac{dq}{q} \int_0^v dx \left[1 + \frac{v^2 - x^2}{2(1 - x^2)} \right] \left(1 - \frac{x^2}{v^2} \right). \end{aligned} \quad (35)$$

After performing the integrals one gets

$$\kappa_T^{\text{LLA}} = \frac{g^2 T m_D^2}{4\pi} \ln \frac{q_{\text{max}}}{m_D} \left[\frac{3}{2} - \frac{1}{2v^2} + \frac{(1-v^2)^2}{4v^3} \ln \frac{1+v}{1-v} \right], \quad (36)$$

again in agreement with the leading log term in Eq. (B32) of Ref. [26]. Note that the transverse momentum diffusion is closely related to the transport coefficient \hat{q} , often entering into the radiative energy loss calculation as a parameter encoding the properties of the medium, and representing the *transverse squared momentum* acquired by the propagating parton *per mean free path* [41]. One can in fact measure the distance X covered in the medium in units of λ_{mfp} , setting $X \equiv n\lambda_{\text{mfp}}$, so that

$$\Delta X \equiv \lambda_{\text{mfp}}. \quad (37)$$

Hence

$$\hat{q} \equiv \frac{\langle \Delta p_T^2 \rangle}{\lambda_{\text{mfp}}} = \left\langle \frac{\Delta p_T^2}{\Delta X} \right\rangle = \frac{1}{v} \left\langle \frac{\Delta p_z^2}{\Delta t} \right\rangle = \frac{2}{v} \kappa_T, \quad (38)$$

leading, in the case of an ultra-relativistic parton, to

$$\hat{q} = \frac{g^2 T m_D^2}{2\pi} \ln \frac{q_{\text{max}}}{m_D}, \quad (39)$$

in agreement with the findings of Ref. [42].

The calculation of the longitudinal momentum diffusion

$$\kappa_L \equiv \left\langle \frac{\Delta p_z^2}{\Delta t} \right\rangle \quad (40)$$

follows in perfect analogy. From

$$\kappa_L = g^2 \int d\omega \int \frac{d\mathbf{q}}{(2\pi)^3} \delta(\omega - \mathbf{q} \cdot \mathbf{v}) \tilde{\rho}(\omega, \mathbf{q}) q^2 \cos^2 \theta N(\omega) \quad (41)$$

one gets

$$\kappa_L = \frac{g^2}{4\pi^2 v} \int_0^{q_{\text{max}}} q dq \int_0^{vq} d\omega \bar{\rho}(\omega, q) \frac{\omega^2}{v^2} \coth \frac{\beta\omega}{2}. \quad (42)$$

Again the result at LLA can be expressed analytically:

$$\begin{aligned} \kappa_L^{\text{LLA}} &= \frac{g^2 T m_D^2}{2\pi v^3} \int_{m_D}^{q_{\text{max}}} \frac{dq}{q^4} \int_0^{vq} d\omega \omega^2 \left[1 + \frac{v^2 - \omega^2/q^2}{2(1 - \omega^2/q^2)} \right] \\ &= \frac{g^2 T m_D^2}{2\pi v^3} \int_{m_D}^{q_{\text{max}}} \frac{dq}{q} \int_0^v dx x^2 \left[1 + \frac{v^2 - x^2}{2(1 - x^2)} \right], \end{aligned} \quad (43)$$

which leads to:

$$\kappa_L^{\text{LLA}} = \frac{g^2 T m_D^2}{4\pi v^2} \ln \frac{q_{\text{max}}}{m_D} \left[1 - \frac{1 - v^2}{2v} \ln \frac{1 + v}{1 - v} \right], \quad (44)$$

to be compared with Eq. (B33) of Ref. [26]. Note that at LLA the relation between friction and momentum-diffusion coefficients, required by the Langevin approach (see Sec. 2 and App. B), holds:

$$\kappa_L^{\text{LLA}} = \frac{2T}{v} \left| \frac{dp}{dt} \right| = \frac{2T}{v} \left| \frac{dE}{dx} \right|_{\text{LLA}} = 2T E \eta_D^{\text{LLA}}, \quad (45)$$

as it can be seen by comparing Eqs. (29) and (44). We notice however that, as it will be discussed in the following, when the strength of the noise depends on the momentum of

the brownian particle (as it turns out to be the case) the viscous term in the Langevin description needs a correction (subleading in T/E) in order to recover the correct continuum limit to the Fokker-Planck equation.

Let us now check *a posteriori* that in a time interval of order τ_{light} the momentum loss Δp and the acquired $\sqrt{\langle p_T^2 \rangle}$ are negligible with respect to the initial $E_p \gg T$, so that the calculation of transport coefficients within the eikonal approach results meaningful.

From $dp/dt = dE/dx$, during the time τ_{light} , one gets:

$$|\Delta p| = \left| \frac{dE}{dx} \right| \tau_{\text{light}} \sim \left| \frac{dE}{dx} \right| D \sim \frac{g^2 m_D^2}{8\pi} \ln \frac{q_{\text{max}}}{m_D} \frac{12\pi T}{g^2 m_D^2 \ln \frac{q_{\text{max}}}{m_D}} \sim T \ll p. \quad (46)$$

Concerning the transverse momentum, during the time interval τ_{light} , one has

$$\langle \Delta p_T^2 \rangle = 2\kappa_T \tau_{\text{light}} \sim \kappa_T D, \quad (47)$$

so that

$$\begin{aligned} \sqrt{\langle \Delta p_T^2 \rangle} &\sim \left(\frac{g^2 T m_D^2}{4\pi} \ln \frac{q_{\text{max}}}{m_D} \frac{12\pi T}{g^2 m_D^2 \ln \frac{q_{\text{max}}}{m_D}} \right)^{1/2} \\ &\sim T \ll p. \end{aligned} \quad (48)$$

4. Transport properties for a $Q\bar{Q}$ pair

Within the same framework it is possible to study the transport properties of a quarkonium, which we simply model as a $Q\bar{Q}$ pair, of a fixed size, propagating with velocity \mathbf{v} in a hot plasma. Similar studies, limited to the energy-loss problem and to the definition of a “dipole potential”, can be found in Refs. [34, 36]. Here the problem is addressed by solving the Maxwell equations in the linear response approximation for a $Q\bar{Q}$ pair (playing the role of an external current) propagating in the QGP, modeled as a dielectric medium.

Clearly, the results will depend not only on the size of the “dipole”, but also on its orientation with respect to the direction of propagation. Following the choice adopted in Ref. [36], we take, without loss of generality, \mathbf{v} along the z -axis, $\mathbf{r} \equiv (r_\perp, 0, z)$ in the zx -plane and the exchanged momentum as $\mathbf{q} = q(\sin \theta \cos \phi, \sin \theta \sin \phi, \cos \theta)$.

We consider then the creation of a quark at $(0, \mathbf{r}'_1)$ and of an anti-quark at $(0, \mathbf{r}'_2)$, with $\mathbf{r} \equiv \mathbf{r}'_1 - \mathbf{r}'_2$, and we follow the propagation of this pair within the eikonal approximation, as already done for the single particle case in Sec. 3. Hence, one can take advantage of Eq. (18), where now the current describes the propagation of a dipole and is given by,

$$J^\mu(x) = g\theta(x^0)\theta(t-x^0) [\delta(\mathbf{x} - \mathbf{r}'_1 - \mathbf{v}x^0) - \delta(\mathbf{x} - \mathbf{r}'_2 - \mathbf{v}x^0)] (1, \mathbf{v}), \quad (49)$$

so that for the $Q\bar{Q}$ propagator one gets:

$$\begin{aligned} \bar{G}(t) &= \exp \left\{ ig^2 \int \frac{d\omega}{2\pi} \int \frac{d\mathbf{q}}{(2\pi)^3} \frac{2[(1 - \cos(\omega - \mathbf{q} \cdot \mathbf{v})t]}{(\omega - \mathbf{q} \cdot \mathbf{v})^2} \right. \\ &\quad \left. \times [1 - \cos(\mathbf{q} \cdot \mathbf{r})] [D_L(\omega, q) + v^2 (1 - (\hat{\mathbf{v}} \cdot \hat{\mathbf{q}})^2) D_T(\omega, q)] \right\}. \end{aligned} \quad (50)$$

One can again consider the large-time decay of the above correlator, which allows to identify the interaction rate of the dipole:

$$\Gamma = 2g^2 \int d\omega \int \frac{d\mathbf{q}}{(2\pi)^3} [1 - \cos(\mathbf{q} \cdot \mathbf{r})] \delta(\omega - \mathbf{q} \cdot \mathbf{v}) \tilde{\rho}(\omega, \mathbf{q}) N(\omega). \quad (51)$$

The Dirac delta can be used to perform the integral over the polar angle, while the azimuthal integration gives rise to a Bessel function, by exploiting the integral representation

$$J_0(q_\perp r_\perp) = \int_0^{2\pi} \frac{d\phi}{2\pi} e^{iq_\perp r_\perp \cos \phi}, \quad (52)$$

with $q_\perp \equiv q \sin \theta$. One can then study the transport properties for the $Q\bar{Q}$ pair.

We first examine the energy loss which is given by [see Eq. (27)]:

$$-\frac{dE}{dx} = \frac{g^2}{2\pi^2 v^2} \int_0^{q_{\max}} q dq \int_0^{qv} d\omega \left[1 - J_0 \left(qr_\perp \sqrt{1 - \frac{\omega^2}{q^2 v^2}} \right) \cos \left(\frac{z\omega}{v} \right) \right] \tilde{\rho}(\omega, q) \omega. \quad (53)$$

For the transverse and longitudinal momentum diffusion coefficients one gets

$$\begin{aligned} \kappa_T &= \frac{g^2}{4\pi^2 v} \int_0^{q_{\max}} q dq \int_0^{qv} d\omega \left[1 - J_0 \left(qr_\perp \sqrt{1 - \frac{\omega^2}{q^2 v^2}} \right) \cos \left(\frac{z\omega}{v} \right) \right] \\ &\quad \times \tilde{\rho}(\omega, q) \coth \left(\frac{\beta\omega}{2} \right) q^2 \left(1 - \frac{\omega^2}{q^2 v^2} \right) \end{aligned} \quad (54)$$

and

$$\begin{aligned} \kappa_L &= \frac{g^2}{2\pi^2 v} \int_0^{q_{\max}} q dq \int_0^{qv} d\omega \left[1 - J_0 \left(qr_\perp \sqrt{1 - \frac{\omega^2}{q^2 v^2}} \right) \cos \left(\frac{z\omega}{v} \right) \right] \\ &\quad \times \tilde{\rho}(\omega, q) \coth \left(\frac{\beta\omega}{2} \right) \frac{\omega^2}{v^2}, \end{aligned} \quad (55)$$

respectively.

In the calculation one also needs to account for the dependence on the dipole orientation. For this purpose we start by considering the *rest frame of the propagating pair* (whose coordinates we label with a tilde): for a S -wave state (till very large velocities the in-medium potential is still approximately spherically symmetric [43]) one has

$$R^2 = \langle \tilde{x}^2 \rangle + \langle \tilde{y}^2 \rangle + \langle \tilde{z}^2 \rangle.$$

Moving then to the *rest frame of the thermal bath* (the laboratory frame), if the pair propagates along the z -axis, its transverse size (in the xy -plane) is not affected and one has:

$$r_\perp \equiv \sqrt{\langle x^2 \rangle + \langle y^2 \rangle} = \sqrt{\langle \tilde{x}^2 \rangle + \langle \tilde{y}^2 \rangle} = \sqrt{2/3} R.$$

On the other hand, the longitudinal size of the dipole turns out to be Lorentz-contracted, according to the relation

$$z = \tilde{z}/\gamma = R/(\sqrt{3}\gamma). \quad (56)$$

The above expressions of r_\perp and z will be employed in the calculation of the transport coefficients.

The small dipole limit can be easily estimated by considering the expansion

$$\begin{aligned} 1 - J_0(qr_\perp \sin \theta) \cos(qz \cos \theta) &\underset{R \ll q_{\max}^{-1}}{\sim} \frac{q^2 r_\perp^2 \sin^2 \theta}{4} + \frac{q^2 z^2 \cos^2 \theta}{2} \\ &= \frac{q^2 R^2}{6} \left(\sin^2 \theta + \frac{\cos^2 \theta}{\gamma^2} \right); \end{aligned} \quad (57)$$

hence, for small sizes, the transport coefficients grow linearly with the transverse area of the dipole. One gets then, in the limits of very small and very large velocities,

$$\begin{aligned} \left\langle -\frac{dE}{dx} \right\rangle_{v \ll 1} &\underset{R \ll q_{\max}^{-1}}{\sim} \frac{g^2 R^2}{12\pi^2 v^2} \int_0^{q_{\max}} q^3 dq \int_0^{qv} d\omega \bar{\rho}(\omega, q) \omega \\ \left\langle -\frac{dE}{dx} \right\rangle_{v \rightarrow 1} &\underset{R \ll q_{\max}^{-1}}{\sim} \frac{g^2 R^2}{12\pi^2} \int_0^{q_{\max}} q^3 dq \int_0^q d\omega \bar{\rho}(\omega, q) \left(1 - \frac{\omega^2}{q^2} \right) \omega \end{aligned} \quad (58)$$

for the energy loss,

$$\begin{aligned} \langle \kappa_T \rangle_{v \ll 1} &\underset{R \ll q_{\max}^{-1}}{\sim} \frac{g^2 R^2}{24\pi^2 v} \int_0^{q_{\max}} q^3 dq \int_0^{qv} d\omega \bar{\rho}(\omega, q) \coth\left(\frac{\beta\omega}{2}\right) q^2 \left(1 - \frac{\omega^2}{q^2 v^2} \right) \\ \langle \kappa_T \rangle_{v \rightarrow 1} &\underset{R \ll q_{\max}^{-1}}{\sim} \frac{g^2 R^2}{24\pi^2} \int_0^{q_{\max}} q^3 dq \int_0^q d\omega \bar{\rho}(\omega, q) \coth\left(\frac{\beta\omega}{2}\right) q^2 \left(1 - \frac{\omega^2}{q^2} \right)^2 \end{aligned} \quad (59)$$

and

$$\begin{aligned} \langle \kappa_L \rangle_{v \ll 1} &\underset{R \ll q_{\max}^{-1}}{\sim} \frac{g^2 R^2}{12\pi^2 v} \int_0^{q_{\max}} q^3 dq \int_0^{qv} d\omega \bar{\rho}(\omega, q) \coth\left(\frac{\beta\omega}{2}\right) \frac{\omega^2}{v^2} \\ \langle \kappa_L \rangle_{v \rightarrow 1} &\underset{R \ll q_{\max}^{-1}}{\sim} \frac{g^2 R^2}{12\pi^2 v} \int_0^{q_{\max}} q^3 dq \int_0^q d\omega \bar{\rho}(\omega, q) \coth\left(\frac{\beta\omega}{2}\right) \omega^2 \left(1 - \frac{\omega^2}{q^2} \right), \end{aligned} \quad (60)$$

for the transverse and longitudinal momentum diffusion coefficients, respectively. Notice that for $v \rightarrow 1$ terms containing z are neglected, since they are suppressed by the Lorenz γ factor: in the ultra-relativistic limit only the transverse area is relevant for the transport properties. In practice, however, the above expansions are not so useful, since the results depend quadratically on the momentum cutoff q_{\max} , which is not well determined and gives a huge systematic theoretical uncertainty. On the contrary working with the exact formulas provides transport coefficients with only a mild logarithmic dependence on the ultraviolet cutoff.

5. Numerical results

Here we present our numerical results, starting from the transport coefficients $\kappa_T(p)$ and $\kappa_L(p)$ introduced in Secs. 3 and 4; they are then employed in the Langevin evolution of the momenta of a large sample of heavy quarks (charm and bottom). The rigorous

results obtained in Sec. 3 are generalized to the QCD case by adding a color charge to the current given in Eq. (19), setting

$$J^{\mu a}(x) = q^a g \theta(x^0) \theta(t - x^0) \delta(\mathbf{x} - \mathbf{r}'_1 - \mathbf{v}x^0)(1, \mathbf{v}), \quad (61)$$

with $a = 1, \dots, N_c^2 - 1$; the corresponding transport coefficients can be simply obtained by multiplying the ones derived in Sec. 3 by the Casimir factor $C_F \equiv q^a q^a$. In the present exploratory study the QGP is modeled as a uniform static medium, considered at different temperatures spanning a range of interest for heavy ion collision experiments.

As already mentioned, the results obtained within the present framework display a logarithmic dependence on the ultraviolet cutoff q_{\max} , related to the maximum momentum exchanged in a collision with a typical thermal particle. Actually, this represents an intrinsic uncertainty of our scheme, which — in dealing with large momentum transfer processes — should be supplemented by a microscopic kinetic calculation involving the evaluation of the Born matrix elements for the scattering of the heavy quarks with the particles of the medium [26, 39, 40]. However, for the sake of ease and consistency we prefer to pursue the approach developed in Sec. 3: indeed, it is able to catch all the essential qualitative features of the transport coefficients (e.g. the growth of $\kappa_{T/L}$ with the momentum p , its suppression in the quarkonium case, etc.) and is simple enough (also in view of a more realistic study of an expanding medium) to be implemented into a Langevin simulation. Bearing in mind that the ambiguity related to the choice of q_{\max} is unavoidable, we refer the reader to Appendix C for details on the procedure employed by us to fix a realistic value for it.

Concerning the value of α_s , which one expects to be quite large at RHIC and to approach a weak-coupling regime at the (larger) LHC temperatures, it has been taken from the 2-loop QCD β -function with the parameters given in Ref. [44]. One has

$$g^{-2}(\mu) = 2 b_0 \ln(\mu/\Lambda_{\text{QCD}}) + \frac{b_1}{b_0} \ln[2 \ln(\mu/\Lambda_{\text{QCD}})], \quad (62)$$

with

$$b_0 = \frac{1}{16\pi^2} \left(11 - \frac{2}{3} N_f \right), \quad b_1 = \frac{1}{(16\pi^2)^2} \left(102 - \frac{38}{3} N_f \right) \quad (63)$$

and $\Lambda_{\text{QCD}} = 261$ MeV. The QCD coupling was then evaluated at a scale proportional to the temperature. As two representative cases we present the results corresponding to the typical choices $\mu = \pi T$ and $\mu = 2\pi T$, the differences reflecting the lack of predictivity of the calculation. A more careful study of the running coupling effects (actually in the evaluation of collisional energy-loss) was given in Refs. [45, 46], but this goes beyond the scope of the present analysis.

We also compare our results, both for the transport coefficients and for the Langevin dynamics of the heavy quarks, with the findings provided by the AdS/CFT correspondence, which, for the $\mathcal{N} = 4$ SYM theory, predicts: [13, 14, 15]

$$\begin{aligned} \kappa_T &= \gamma^{1/2} \sqrt{\lambda} \pi T_{\text{SYM}}^3, \\ \kappa_L &= \gamma^{5/2} \sqrt{\lambda} \pi T_{\text{SYM}}^3, \end{aligned} \quad (64)$$

where $\gamma = 1/\sqrt{1-v^2}$ and $\lambda = g_{\text{SYM}}^2 N_c$. Actually, translating the above results to the hot-QCD case is not free of ambiguities and different strategies were proposed. Here we

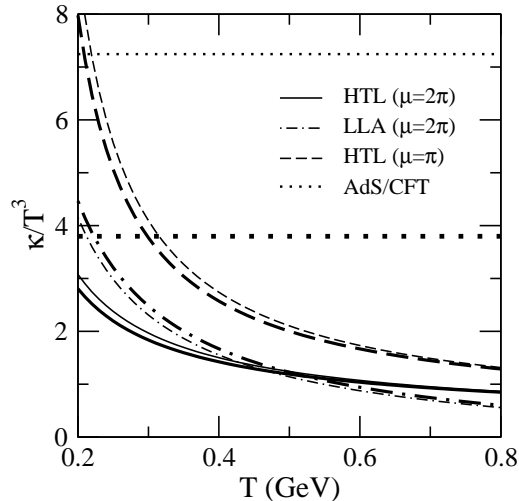


Figure 1: The HTL momentum-diffusion coefficients $\kappa_{T/L}$ divided by T^3 for a bottom quark of mass $M = 4.2$ GeV and momentum $p = 4$ GeV as a function of the temperature. The HTL results, for $\mu = 2\pi$ and $\mu = \pi$, are shown (solid and dashed lines, respectively). The dot-dashed lines correspond to the LLA results. Thick lines refer to κ_T , thin lines to κ_L . The AdS/CFT values are also reported.

follow the recipe adopted in Ref. [14], which is based on matching the energy density and the $Q\bar{Q}$ force in the two theories, namely:

$$3^{1/4}T_{\text{SYM}} = T_{QCD} \quad \text{and} \quad \lambda = 5.5, \quad (65)$$

the latter being chosen within the range $3.5 < \lambda < 8$ allowed by the above mentioned procedure. It was pointed out in Ref. [13] that the results in Eq. (64) only hold for heavy-quark momenta corresponding to γ factors below a critical limit:

$$\gamma < \gamma_c \equiv \left(\frac{M}{\sqrt{\lambda}T_{\text{SYM}}} \right)^2. \quad (66)$$

To our knowledge no calculation is available for larger momenta. Hence, in our plots, as γ exceeds this critical value, we freeze κ_T and κ_L to their estimates below γ_c . Had we trivially identified the coupling and the temperature in the two theories, requiring $\lambda = 6\pi$ to reproduce a QCD plasma with $N_c = 3$ and $\alpha_s = g^2/4\pi \approx 0.5$, the range of validity of the AdS/CFT calculation would have been even more limited.

In the range of temperatures covered by our analysis the transport coefficients $\kappa_{T/L}$ change dramatically, increasing approximately as T^3 (deviations being due to running-coupling effects), as it is displayed in Fig. 1. This leads to observable consequences for the heavy-quark dynamics, that we will discuss. Fig. 1 refers to the case of a b -quark of not too large momentum, so that the condition in Eq. (66) is satisfied. In the same figure we also show for comparison the LLA result for $\mu = 2\pi$.

In Fig. 2 we give, for a charm quark and for different temperatures, the coefficients $\kappa_T(p)$ and $\kappa_L(p)$ which are derived from our HTL calculation. We also display, for

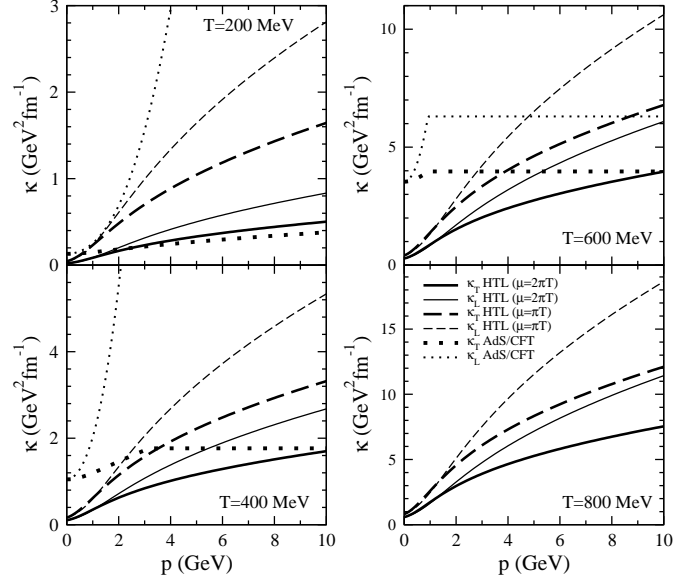


Figure 2: The HTL momentum-diffusion coefficients $\kappa_{T/L}(p)$ for a charm quark of mass $M = 1.2$ GeV for a range of temperatures above T_c of experimental interest. We also plot, in the regime where they are available, the AdS/CFT results. Again, thick lines refer to κ_T and thin ones to κ_L .

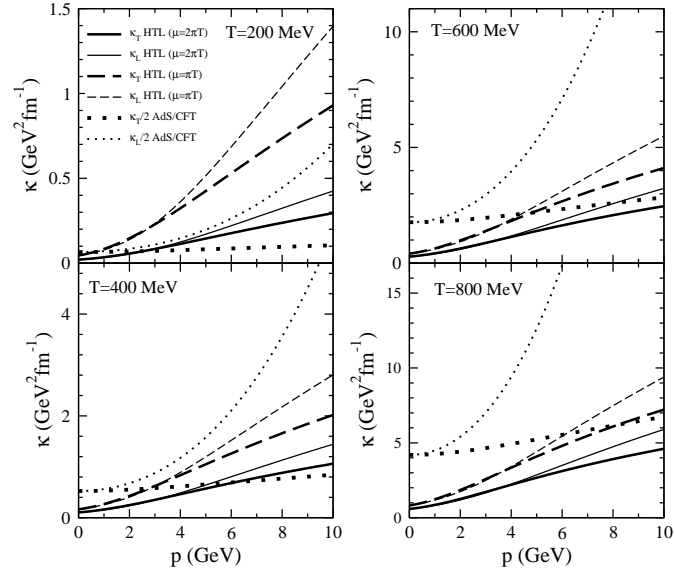


Figure 3: As in Fig. 2, but for a bottom quark of mass $M = 4.2$ GeV.

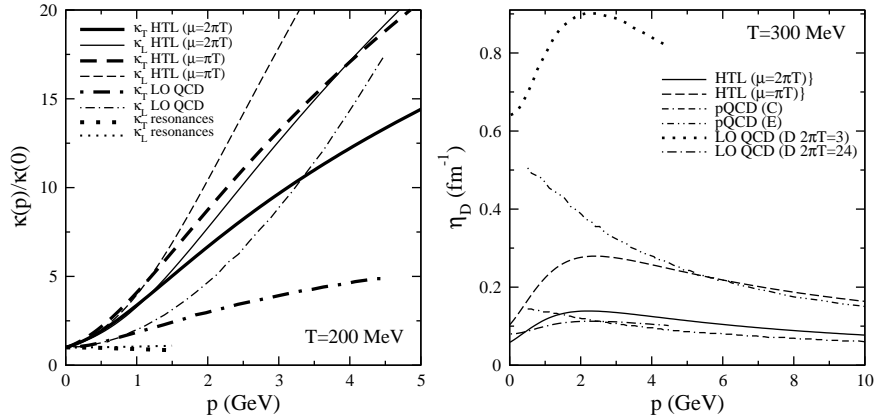


Figure 4: Left panel: $\kappa_{T,L}(p)/\kappa_{T,L}(0)$ as a function of momentum for charm quarks ($m_c = 1.5$ GeV) at $T = 200$ MeV in our model (HTL), in the the QCD kinetic calculation of Ref. [26] (LO QCD) and in the resonance model of Ref. [10]. Right panel: the drag coefficient $\eta_D(p)$ as a function of momentum for charm quarks ($m_c = 1.5$ GeV) at $T = 300$ MeV in our model (HTL), in the calculations of Refs. [18, 20] (pQCD) and [26] (LO QCD).

comparison, the corresponding AdS/CFT result. As expected, the latter model provides stronger coefficients and also a much steeper momentum dependence of $\kappa_L(p)$. Notice that, for large enough temperatures, $\gamma_c < 1$, so that the condition $\gamma < \gamma_c$ cannot be satisfied. In Fig. 3 the same quantities for the case of a bottom quark are shown.

In Fig. 4 we compare our results to a few of the calculations for the transport coefficients available in the literature. In the left panel we display the ratios $\kappa_{T,L}(p)/\kappa_{T,L}(0)$ at $T = 200$ MeV in our HTL model together with the QCD kinetic calculation of Ref. [26] (LO QCD) and the resonance model of Ref. [10]. The momentum dependence of the longitudinal coefficient has on the whole a similar trend in the HTL and LO QCD models, whereas in the latter the transverse coefficient displays a less pronounced momentum dependence. On the other hand, the resonance model provides coefficients that are essentially flat in the available range of momenta.

In the right panel of Fig. 4 we compare the drag coefficient η_D as obtained in the HTL model at $T = 300$ MeV to the LO QCD model of Ref. [26]. In that model the value of $\eta_D(0)$ is parameterized through the diffusion constant in space D , which is treated as a free parameter, and in the figure we display two choices for D in the range considered in Ref. [26]. As one can see, the momentum dependence is similar to the one of the HTL model, the absolute normalization covering a wider range of values.

In the same panel we also report the results obtained in Refs. [18, 20], where an emended perturbative QCD (pQCD) calculation is employed by introducing a smaller infrared regulator and a suitably chosen running coupling constant. In the figure the labels (C) and (E) refer to two different choices of parameters (see Table I of Ref. [18]). The coefficient η_D is smoothly decreasing with p in this model, whereas in the HTL model (and also in the LO QCD one) it displays a maximum. At momenta $p \gtrsim 3$ GeV the magnitude of η_D is similar in the HTL and pQCD calculations, the latter, on the other hand, being definitely larger at small momenta. Also the resonance model of Ref. [10]

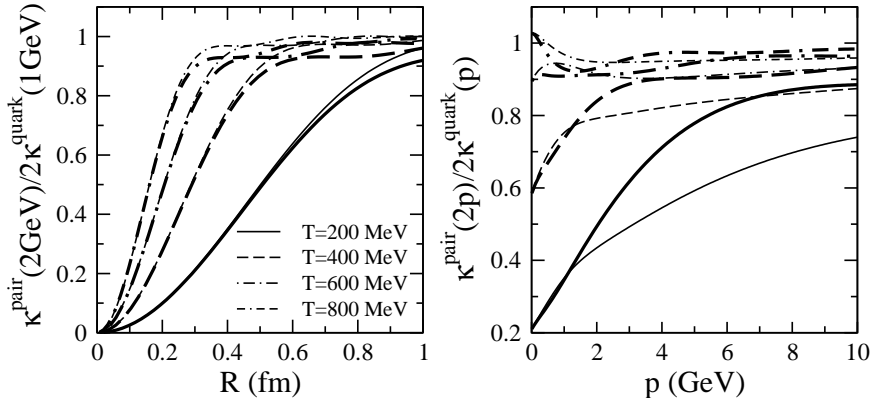


Figure 5: The charmonium transport coefficients, normalized to the result for two independent c -quarks. Left panel: as a function of the $Q\bar{Q}$ separation, for a pair propagating with momentum $p_{c\bar{c}} = 2p_c = 2$ GeV. Right panel: as a function of the quark momentum, for a pair of size $R = 0.4$ fm. Thick lines refer to κ_T , thin lines to κ_L . Various temperatures are considered.

displays a smoothly decreasing behavior with momentum.

We then consider, in Figs. 5 and 6, the case of a $Q\bar{Q}$ pair crossing the QGP. The quarkonium is modeled as a pair of heavy quarks, which propagates in the medium with a fixed separation and with a momentum given by the sum of the two individual quarks. Any binding effect is neglected, hence one has simply

$$\begin{aligned} P_\Phi &= P_Q + P_{\bar{Q}} = (E_p^Q, \mathbf{p}) + (E_p^{\bar{Q}}, \mathbf{p}) = (2E_p^Q, 2\mathbf{p}) \\ &\equiv (E_{2p}^\Phi, 2\mathbf{p}), \end{aligned} \quad (67)$$

with $M_\Phi \equiv 2M_c^{\text{eff}} \approx 2 \cdot 1.5$ GeV in the case of J/ψ and $M_\Phi \equiv 2M_b^{\text{eff}} \approx 2 \cdot 4.7$ GeV in the case of a Υ meson.

In spite of its simplicity such a model is able to display how — due to the destructive interference effect encoded in the $[1 - \cos(\mathbf{q} \cdot \mathbf{r})]$ factor of Eq. (51) — quarkonium states of small size propagating in the QGP would suffer much less rescatterings with respect to two uncorrelated heavy quarks, as it appears from the left panels of Figs. 5 and 6. In particular, since the relevant quantity is the ratio between the average separation R of the heavy quarks and the Debye radius $R_D \equiv m_D^{-1}$, for a given dipole size the suppression is more dramatic at small temperatures, where the Debye radius is larger, implying a smaller value of R/R_D .

In the right panels we still consider the quarkonium transport coefficients, but as a function of the momentum p of the single “constituent” heavy quark. We take $R = 0.4$ fm in Fig. 5 and $R = 0.2$ fm in Fig. 6, corresponding to the typical mean square radius of the charmonium and bottomonium ground states, respectively.

We now make use of the above findings for $\kappa_{T/L}(p)$ to follow the relaxation to thermal equilibrium of a large sample of charm or bottom quarks. We model such a process with the following Langevin equation:

$$\frac{dp^i}{dt} = -\eta_D(p)p^i + \xi^i(t). \quad (68)$$

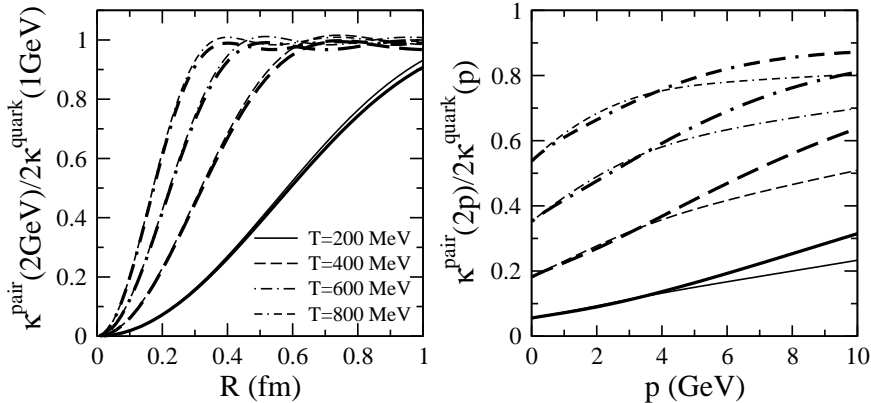


Figure 6: The bottomonium transport coefficients, normalized to the result for two independent b -quarks. Left panel: as a function of the $Q\bar{Q}$ separation, for a pair propagating with momentum $p_{b\bar{b}} = 2p_b = 2$ GeV. Right panel: as a function of the quark momentum, for a pair of size $R = 0.2$ fm. Thick lines refer to κ_T , thin lines to κ_L . Various temperatures are considered.

As in the non-relativistic case introduced in Sec. 2, the resulting stochastic evolution of the heavy-quark momenta is determined by the noise correlation function

$$\langle \xi^i(t) \xi^j(t') \rangle = \delta(t - t') [\kappa_L(p) \hat{p}^i \hat{p}^j + \kappa_T(p) (\delta^{ij} - \hat{p}^i \hat{p}^j)], \quad (69)$$

which is expressed in terms of the transverse and longitudinal transport coefficients previously evaluated. In Eq. (68) the drag coefficients $\eta_D(p)$ is fixed in order to ensure the approach to equilibrium. An extended discussion of the relativistic Langevin equation, of its discretization and of the algorithm employed in its numerical implementation is reported in Appendix B. We mention here that other choices can be found in the literature. Some authors, for instance, performed a first-principle calculation for η_D [29], fixing the remaining coefficients by requiring the proper equilibrium limit. Our choice is motivated both by the quest for consistency (since the same microscopic calculation provides both κ_T and κ_L) and by the importance of distinguishing between the transverse and longitudinal momentum broadening of a fast particle (at variance with what done in [29]). Finally, we observe that, in any case, in dealing with a stochastic differential equation, the – momentum-dependent – friction coefficient receives a correction depending on the adopted discretization scheme, so that it appears more natural to fix the latter “by hand”. We point out, however, that the HTL calculation, at least at LLA, provides consistent results for η_D and κ_L .

We start with the case of a sample of $2 \cdot 10^6$ charm quarks, with an initial momentum p_0 representative of their typical initial p_T in nucleus-nucleus collisions. The parametrization of their spectrum used in Ref. [26], referring to RHIC conditions, gives, for instance, $\bar{p}_T = 1.23$ GeV. In the case of Pb-Pb collisions at LHC (at $\sqrt{s_{NN}} = 5.5$ TeV), one gets, instead, $\bar{p}_T = 2.18$ GeV [21] for charm quarks generated by PYTHIA with parameters tuned to reproduce the results by Mangano et al. [47]. The momentum distributions resulting from the Langevin evolution, for different values of T and p_0 , are presented in Figs. 7 and 8, for c -quarks at increasing values of time. For any value of

T , for large enough times, the charm momenta turn out to be described by a relativistic Maxwell-Jüttner distribution

$$f_{\text{MJ}}(p) \equiv \frac{e^{-E_p/T}}{4\pi M^2 T K_2(M/T)}, \text{ with } \int d^3p f_{\text{MJ}}(p) = 1, \quad (70)$$

where K_2 is a modified Bessel function. We notice, however, that the approach to equilibrium is much faster for larger values of the temperature, due to the huge increase of the coefficients $\kappa_{T/L}(p)$ with T displayed in Fig. 1.

For comparison we also give, in the right panels, the corresponding results arising from the AdS/CFT estimate of the transport coefficients entering into the Langevin equation. Such a strongly-coupled scenario gives rise to an extremely fast relaxation toward equilibrium. Notice that the case $T = 800$ MeV is out of the range of validity of the present available methods to compute $\kappa_{T/L}(p)$ within the SYM framework.

We then consider, for the same range of temperatures, the Langevin dynamics of an ensemble of b -quarks with mass $M = 4.2$ GeV, initialized with a momentum $p_0 = 6$ GeV, chosen of the order of the average p_T of the spectrum generated by PYTHIA, with the parameters given in Ref. [21]. Notably this corresponds to a much harder momentum than the equilibrium value. This fact, together with the larger mass of the bottom quark, makes the approach to equilibrium much slower with respect to the case of charm. Our results for the momentum distribution function are displayed in Fig. 9. As it can be seen the HTL calculation provides relaxation times too large to be of interest for the realistic case of an expanding (and cooling) fireball.

On the contrary the AdS/CFT scenario supports a quite rapid thermalization also for b -quarks, the latter being almost immediate at the largest temperatures examined.

Finally, in order to get a feeling of the rapidity of the thermalization process in the different cases considered here (which can be not so easy to grasp just by looking at the distributions), we give in Figs. 10 and 11 the evolution of the mean squared momentum $\langle p^2 \rangle$ to its equilibrium value predicted by the Maxwell-Jüttner distribution of Eq. (70). The difference between the two models (HTL and SYM) appears particularly evident in the case of b -quarks, which could be an interesting probe to study at LHC in order to discriminate between different scenarios.

6. Discussion and conclusions

The two main issues addressed in this paper are the evaluation of transport coefficients for heavy quarks in the QGP and the study of the resulting Langevin evolution of their momenta. We showed that important qualitative and quantitative (though affected by some systematic uncertainty) information on the energy-loss and momentum-broadening of heavy quarks can be extracted from an approach (based on the HTL approximation) developed for a different purpose, namely for the definition of an effective in-medium potential for a pair of static quarks [22, 23].

Concerning the transport coefficients, both κ_T and κ_L were found to display a sizable growth with the momentum, κ_L increasing faster than κ_T .

The approach developed in this work has been also useful for the study of transport properties of quarkonia. $Q\bar{Q}$ states of small size, behaving as an almost neutral object, turned out to suffer less rescatterings. This could be of phenomenological interest in

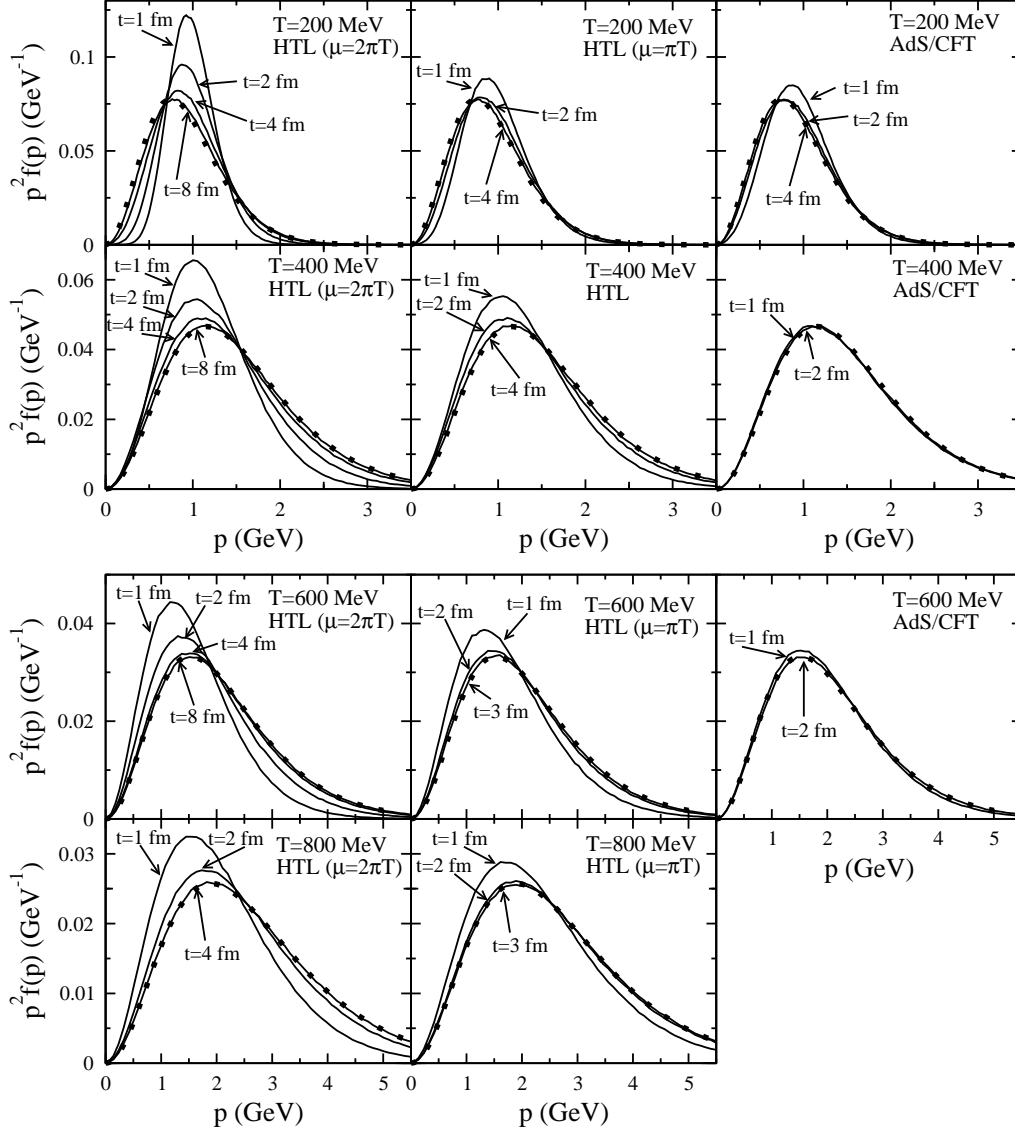


Figure 7: The momentum distribution at different times t of charm quarks with $M = 1.2 \text{ GeV}$ in a QGP for a range of temperatures. The left and central panels display the HTL results ($\mu = 2\pi T$ and $\mu = \pi T$, respectively), while the right panels refer to the AdS/CFT calculation. For the initial momentum we take $p_0 = 1 \text{ GeV}$. Square-dots represent the Maxwell-Jüttner equilibrium distributions.

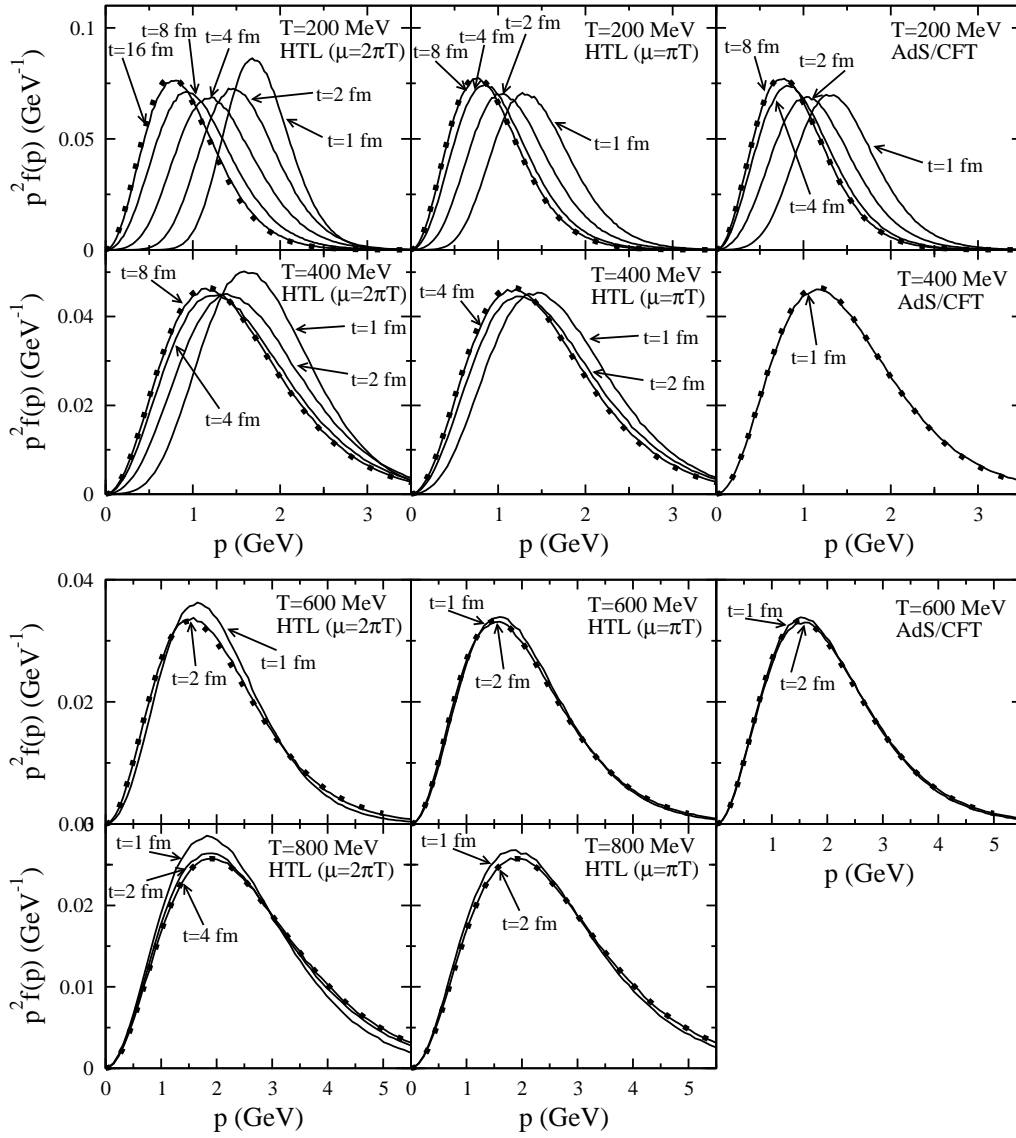


Figure 8: As in Fig. 7, but for an initial momentum $p_0 = 2 \text{ GeV}$.

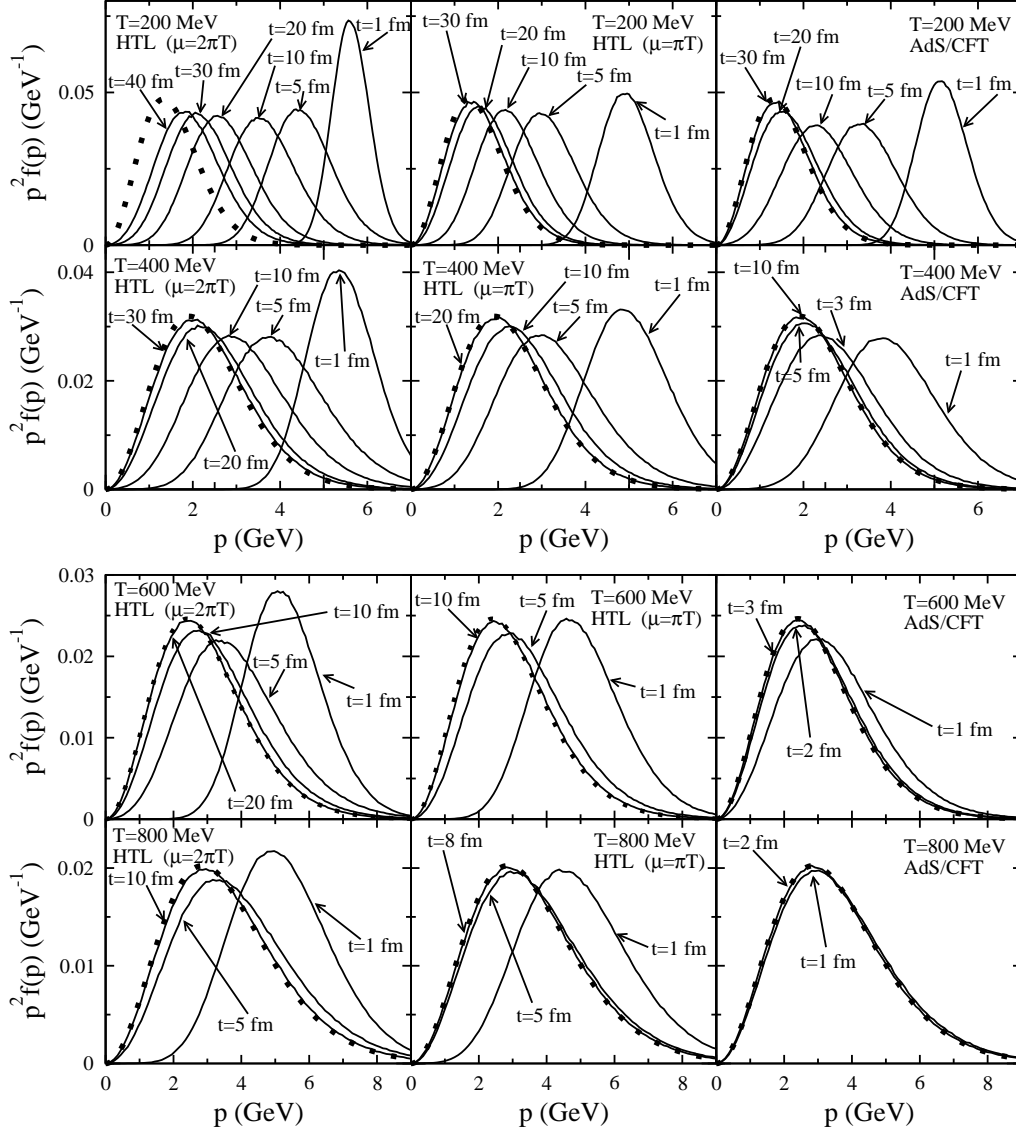


Figure 9: As in Fig. 7, but for a sample of bottom quarks of mass $M = 4.2$ GeV and initial momentum $p_0 = 6$ GeV.

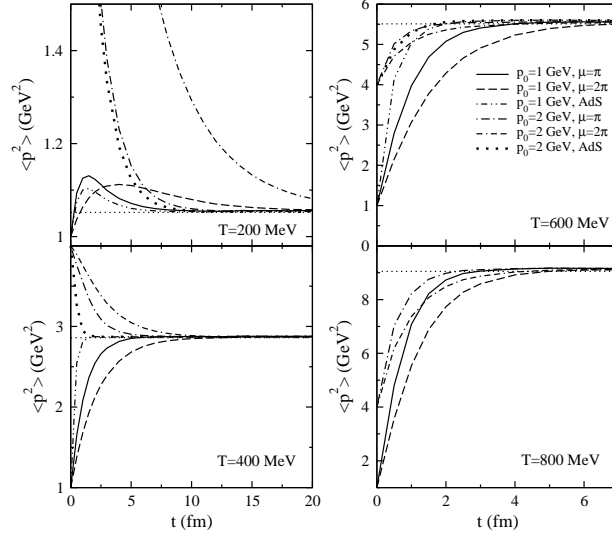


Figure 10: The approach of $\langle p^2 \rangle$ to the equilibrium value predicted by the Maxwell-Jüttner distribution in the case of charm quarks at various temperatures.

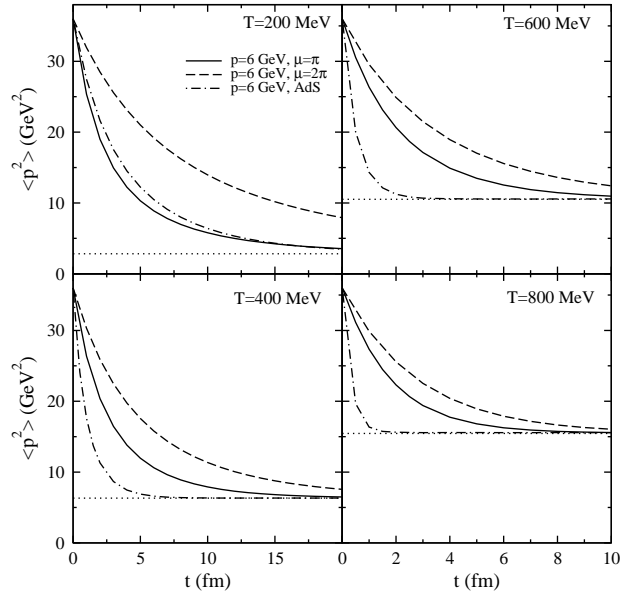


Figure 11: As in Fig. 10, but in the case of bottom quarks.

order to discriminate between different production/suppression scenarios. Analysis of momentum spectra would, in fact, help to understand whether the observed quarkonia in the final state arise from the recombination of uncorrelated heavy quarks or from their primordial production, after crossing unaffected the deconfined environment.

We then addressed the Langevin evolution of a large sample of heavy quarks (charm and bottom) — starting from an initial momentum chosen to be representative of the typical ones in nucleus-nucleus collisions — and following their approach to thermalization. We also tried to give some basic discussion of the essential aspects of the relativistic Langevin equation as an effective model to describe the relaxation of an ensemble of heavy particles toward equilibrium.

Our numerical findings allow to draw some general considerations.

We first notice that at the largest temperatures explored ($T = 600$ and $T = 800$ MeV) the thermalization of c -quarks predicted by our (weak-coupling) HTL calculation is quite fast. Such an occurrence could be of phenomenological interest for LHC, where one expects quite large temperatures to be achieved in the first instants after the collision. On the contrary the relaxation of b -quark spectra toward equilibrium arising from the present HTL calculation is always too slow to allow them to follow the flow of the medium in the realistic case of an expanding fireball.

For what concerns the strongly-coupled AdS/CFT scenario, c -quarks are found to thermalize almost immediately, in spite of our conservative choice of freezing the values of $\kappa_{T/L}$ for $\gamma < \gamma_c$. Interestingly, also b -quarks approach equilibrium quite fast (at the largest temperatures), making possible for them to inherit at least part of the flow of the medium produced in heavy-ion collisions. Elliptic-flow is in fact expected to develop in the very initial stage of the fireball evolution, when the medium is extremely hot, entailing large values of $\kappa_{T/L}$ (which, we remind, grow as T^3).

At the large temperatures realized at LHC, b -quarks appear then as a promising probe to discriminate between the weakly and strongly-coupled scenarios. A sizable flow of b -quarks could not be compatible with any weak-coupling perturbative calculation. Measurement of the elliptic-flow and of the quenching of p_T spectra of single-electrons (or positrons) arising from the semi-leptonic decays of B -mesons (which will be possible at LHC) could then shed light on the transport properties of the QGP at the future accessible regime of temperatures.

In future work we plan to employ the approach developed here, whose numerical implementation turns out to be quite inexpensive, in order to address the realistic case of a fireball displaying longitudinal and transverse expansion. Supplementing our study with a more microscopic kinetic calculation of the hard-scattering contribution to the transport coefficients is also object of our current investigation.

Acknowledgments

We are grateful to F. Prino for fruitful discussions and for providing us with the heavy-quark production spectra expected at LHC.

A. The HTL propagators and spectral functions

We give here the explicit expressions for the HTL gluon (photon in QED) propagators in the Coulomb gauge, together with their spectral functions, which are employed

throughout the text. Further details can be found, e.g., in Ref. [48].

The longitudinal and transverse *analytical* (off the real-energy axis) propagators read, respectively,

$$\begin{aligned}\Delta_L(q^0, q) &= \frac{-1}{q^2 + \Pi_L(x)}, \\ \Delta_T(q^0, q) &= \frac{-1}{(q^0)^2 - q^2 - \Pi_T(x)},\end{aligned}\quad (71)$$

where

$$\begin{aligned}\Pi_L(x) &= m_D^2 [1 - Q(x)], \\ \Pi_T(x) &= \frac{m_D^2}{2} [x^2 + (1 - x^2)Q(x)] \quad \text{and} \\ Q(x) &\equiv \frac{x}{2} \ln \frac{x+1}{x-1},\end{aligned}\quad (72)$$

being $x \equiv q^0/q$.

The corresponding *retarded* propagators are obtained by setting $q^0 = \omega + i\eta$ in the above expressions, namely:

$$D_{L/T}^R(\omega, q) \equiv \Delta_{L/T}(\omega + i\eta, q). \quad (73)$$

The HTL gluon (photon) spectral function follows immediately from the definition:

$$\rho_{L/T}(\omega, q) \equiv 2\text{Im}D_{L/T}^R(\omega, q). \quad (74)$$

One gets (for space-like momenta):

$$\begin{aligned}\rho_L(\omega, q) &= \frac{2\pi m_D^2 \frac{\omega}{2q}}{\left[q^2 + m_D^2 \left(1 - \frac{\omega}{2q} \ln \left| \frac{\omega+q}{\omega-q} \right| \right) \right]^2 + \left(\pi m_D^2 \frac{\omega}{2q} \right)^2}, \\ \rho_T(\omega, q) &= \frac{\pi m_D^2 \frac{\omega(q^2 - \omega^2)}{2q^3}}{\left[\omega^2 - q^2 - \frac{m_D^2 \omega^2}{2} \frac{1}{q^2} \left(1 - \frac{\omega^2 - q^2}{2\omega q} \ln \left| \frac{\omega+q}{\omega-q} \right| \right) \right]^2 + \left[\frac{\pi m_D^2 \omega(\omega^2 - q^2)}{2q^3} \right]^2}.\end{aligned}\quad (75)$$

Their expressions at LLA are obtained by neglecting the self-energy corrections in the denominators and are given by:

$$\begin{aligned}\rho_L(\omega, q) &\underset{\text{LLA}}{\sim} \frac{2\pi m_D^2 \frac{\omega}{2q}}{q^4}, \\ \rho_T(\omega, q) &\underset{\text{LLA}}{\sim} \frac{\pi m_D^2 \frac{\omega}{2q}}{q^2(q^2 - \omega^2)}.\end{aligned}\quad (76)$$

This implies that the infrared divergences are no longer screened by the Debye mass, and must be regulated by hand by setting a lower cutoff of order m_D in the integration over the three-momentum of the exchanged gluons (photons).

When dealing with the in-medium heavy quark propagation, within the eikonal approximation, one needs to consider the exponentiation of the *real-time* gauge-field propagator; the latter is given by

$$\begin{aligned} D_L(\omega, q) &= -\frac{1}{q^2} + \int_{-\infty}^{+\infty} \frac{dq^0}{2\pi} \frac{\rho_L(q^0, q)}{q^0 - (\omega + i\eta)} + i\rho_L(\omega, q)N(\omega) \\ D_T(\omega, q) &= \int_{-\infty}^{+\infty} \frac{dq^0}{2\pi} \frac{\rho_T(q^0, q)}{q^0 - (\omega + i\eta)} + i\rho_T(\omega, q)N(\omega), \end{aligned} \quad (77)$$

where $N(\omega)$ is the customary Bose distribution. The above expressions are related to the respective retarded propagators as follows:

$$\begin{aligned} D_{L/T}(\omega, q) &= D_{L/T}^R(\omega, q) + i\rho_{L/T}(\omega, q)N(\omega) \\ &= \text{Re} D_{L/T}^R(\omega, q) + i \left(N(\omega) + \frac{1}{2} \right) \rho_{L/T}(\omega, q). \end{aligned} \quad (78)$$

B. The relativistic Langevin equation

In Sec. 2 we discussed the non-relativistic Langevin dynamics of a heavy-quark in a hot plasma. This allowed us to take advantage of well known results like the Einstein relation given in Eq. (10), which provides a link between the friction and the momentum-diffusion coefficients and can be seen as an example of the fluctuation-dissipation theorem.

The generalization of the Langevin equation to the relativistic case is far from trivial. In particular one can no longer ignore the momentum dependence of the transport coefficients, as it is usually done in non-relativistic studies; in turn, this introduces in the definition of the friction term a dependence on the adopted discretization scheme.

From the mathematical point of view the relativistic Langevin equation belongs to the class of *stochastic differential equations* with multiplicative noise, which represents by itself an active field of investigation [49]. Although the traditional Langevin treatment of non-equilibrium dynamics is textbook material, the case of state-dependent (momentum dependent in the present case) transport coefficients has been only rarely considered in the literature [26, 27, 28, 29, 50, 51, 52] and from quite different perspectives. Hence we provide in this Appendix a self-contained discussion of the essential aspects of the relativistic Langevin equation. We mainly follow the approach presented in Ref. [52], which we found particularly clear.

For simplicity, let us consider the one-dimensional case, which is sufficient to illustrate the relevant conceptual points. The generalization to the realistic d -dimensional case will follow immediately. Also in the relativistic case one postulates that the momentum of an external particle placed in a hot medium evolves according to the equation

$$\frac{dp}{dt} = -\eta_D(p)p + \xi(t), \quad (79)$$

where the right hand side is given again by the sum of a friction force and a term related to the random momentum kicks received from the medium particles

$$\langle \xi(t)\xi(t') \rangle = \kappa(p)\delta(t - t'), \quad (80)$$

still assumed to be uncorrelated. This is expressed by the delta function, leading to a flat power spectrum referred to as *white noise*; however the strength κ of the noise in Eq. (80) depends, in the general case, on the momentum of the brownian particle (*multiplicative noise*). One can factor out the momentum dependence by defining $g(p) \equiv \sqrt{\kappa(p)}$, so that Eq. (79) becomes

$$\frac{dp}{dt} = -\eta_D(p)p + g(p)\eta(t), \quad (81)$$

with

$$\langle \eta(t)\eta(t') \rangle = \delta(t - t'). \quad (82)$$

We anticipate that the expression of the friction coefficient $\eta_D(p)$ will depend on the discretization scheme, namely on the value of p at which in the discretized equation (employed in the numerical simulations)

$$\Delta p \equiv p(t + \Delta t) - p(t) = -[\eta_D(p)p]\Delta t + g(p)\eta(t)\Delta t \quad (83)$$

the terms in the right hand side must be evaluated. In the following we wish to clarify this point.

The Langevin equation can be written in the general form

$$\frac{dp}{dt} = f(p) + g(p)\eta(t), \quad (84)$$

where we can identify

$$\begin{aligned} f(p) &\equiv -\eta_D(p)p \equiv -\eta_D^{(0)}(p)p + f_1(p) \\ &= -\left[\eta_D^{(0)}(p) - \frac{f_1(p)}{p} \right] p. \end{aligned} \quad (85)$$

In the above the friction coefficient has been written as the sum of a leading term, linked to the momentum diffusion coefficient $\kappa(p)$ by a relation analogous to the one occurring in the non-relativistic case, and a subleading (in T/E) correction which will depend on the discretization procedure. The ambiguity will be eliminated by requiring that in the continuum limit all the different discretization schemes yield to the same Fokker-Planck equation for the momentum distribution, which admits the equilibrium distribution $\exp(-E_p/T)$ as a steady solution.

We start by integrating Eq. (84), which leads to the formal expression

$$p(t + \Delta t) - p(t) = \int_t^{t+\Delta t} ds [f(p(s)) + g(p(s))\eta(s)]. \quad (86)$$

However the random noise term $\eta(s)$ makes the value of the integral ambiguous and a recipe has to be given to evaluate the right hand side of the above equation. One can overcome this difficulty by considering a whole family of different discretizations, labeled by a parameter $\alpha \in [0, 1]$, such that

$$\Delta p = f[p(t) + \alpha\Delta p]\Delta t + g[p(t) + \alpha\Delta p] \int_t^{t+\Delta t} ds \eta(s). \quad (87)$$

Note that the momentum increment Δp arises from the sum of a deterministic friction term of order Δt and of a random term of order $\sqrt{\Delta t}$. After defining $p_0 \equiv p(t)$, the first term in the above, being already of order Δt , can be evaluated at p_0 , while for the second term it is useful to expand

$$g[p_0 + \alpha\Delta p] = g(p_0) + g'(p_0)\alpha\Delta p + \dots, \quad (88)$$

where the last term, multiplying the noise-integral, provides also a contribution of order Δt . Taking advantage of the fact that $\langle \eta(s) \rangle = 0$ and of Eq. (82) one immediately gets:

$$\langle \Delta p \rangle = f(p_0)\Delta t + \alpha g(p_0)g'(p_0)\Delta t \quad (89)$$

and

$$\langle (\Delta p)^2 \rangle = g^2(p_0)\Delta t. \quad (90)$$

We now consider the link between the Langevin equation and the Fokker-Planck equation for the momentum distribution $P(p, t)$ of the brownian particles. For the latter the following equation holds:

$$P(p, t + \Delta t) = \int_{-\infty}^{+\infty} dp_0 P(p, t + \Delta t | p_0, t) P(p_0, t), \quad (91)$$

where $P(p, t + \Delta t | p_0, t)$ represents the *conditional probability* that a particle with momentum p_0 at time t will be found with momentum p at time $t + \Delta t$. One can identify such a conditional probability with the following expectation value over the ensemble of brownian particles:

$$\begin{aligned} P(p, t + \Delta t | p_0, t) &\equiv \langle \delta[p - p(t + \Delta t)] \rangle_{p_0, t} \\ &= \langle \delta[p - p_0 - \Delta p] \rangle_{p_0, t}, \end{aligned} \quad (92)$$

with Δp taken from the Langevin equation (87). One can then expand up to second order, obtaining:

$$P(p, t + \Delta t | p_0, t) = \delta(p - p_0) - \langle \Delta p \rangle \frac{\partial}{\partial p} \delta(p - p_0) + \frac{1}{2} \langle (\Delta p)^2 \rangle \frac{\partial^2}{\partial p^2} \delta(p - p_0) + \dots \quad (93)$$

After inserting the above expansion into Eq. (91) and exploiting Eqs. (89) and (90), one arrives to the Fokker-Planck equation:

$$\begin{aligned} \frac{\partial}{\partial t} P(p, t) &= \frac{\partial}{\partial p} \left[-f(p) - \alpha g(p)g'(p) + \frac{1}{2} \frac{\partial}{\partial p} g^2(p) \right] P(p, t) \\ &= \frac{\partial}{\partial p} \left[\eta_D^{(0)}(p)p - f_1(p) - \alpha g(p)g'(p) + \frac{1}{2} \frac{\partial}{\partial p} g^2(p) \right] P(p, t) \\ &= \frac{\partial}{\partial p} \left[\eta_D^{(0)}(p)p - f_1(p) + \frac{1}{2}(1 - \alpha)\kappa'(p) + \frac{1}{2}\kappa(p) \frac{\partial}{\partial p} \right] P(p, t). \end{aligned} \quad (94)$$

Then, the requirement that the above equation is independent of the discretization scheme (i.e. of α) and admits the steady solution $\exp(-E_p/T)$, with $E_p \equiv \sqrt{p^2 + M^2}$,

allows to fix in an unambiguous way $\eta_D^{(0)}(p)$ and $f_1(p)$. One gets:

$$\eta_D^{(0)}(p) = \frac{\kappa(p)}{2TE_p} \quad (95)$$

$$f_1(p) = \frac{1}{2}(1 - \alpha)\partial_p\kappa(p). \quad (96)$$

Hence the friction coefficient to be employed in the numerical Langevin simulations depends on the discretization scheme through the parameter α and reads:

$$\eta_D(p) = \frac{\kappa(p)}{2TE_p} - \frac{1}{2}(1 - \alpha)\frac{\partial_p\kappa(p)}{p}. \quad (97)$$

Two very popular choices in the literature are $\alpha = 0$ (Ito discretization) and $\alpha = 1/2$ (Stratonovich discretization). For our purposes it will result more convenient to keep track of the dependence on the velocity of the brownian particle $v = p/E_p$ rather than on its momentum, so that:

$$\eta_D(v) = \frac{\kappa(v)}{2TE_p} - \frac{1}{2}(1 - \alpha)\frac{1 - v^2}{pE_p}\partial_v\kappa(v). \quad (98)$$

We notice that the Fokker-Planck equation turns out to be completely determined by the momentum-diffusion coefficient:

$$\frac{\partial}{\partial t}P(p, t) = \frac{\partial}{\partial p} \left\{ \frac{1}{2}\kappa(p) \left[\frac{p}{TE_p} + \frac{\partial}{\partial p} \right] P(p, t) \right\}. \quad (99)$$

We now consider the relativistic brownian motion in d space dimensions. The Langevin equation in this case reads:

$$\frac{dp^i}{dt} = -\eta_D(p)p^i + \xi^i(t), \quad (100)$$

with

$$\langle \xi^i(t)\xi^j(t') \rangle = b^{ij}(\mathbf{p})\delta(t - t'), \quad (101)$$

where

$$b^{ij}(\mathbf{p}) \equiv \kappa_L(p)\hat{p}^i\hat{p}^j + \kappa_T(p)(\delta^{ij} - \hat{p}^i\hat{p}^j). \quad (102)$$

It is also useful to introduce the tensor

$$\begin{aligned} g^{ij}(\mathbf{p}) &\equiv \sqrt{\kappa_L(p)}\hat{p}^i\hat{p}^j + \sqrt{\kappa_T(p)}(\delta^{ij} - \hat{p}^i\hat{p}^j) \\ &\equiv g_L(p)\hat{p}^i\hat{p}^j + g_T(p)(\delta^{ij} - \hat{p}^i\hat{p}^j). \end{aligned} \quad (103)$$

This allows one to factor out the momentum dependence of the noise term in Eq. (100), which becomes

$$\frac{dp^i}{dt} = -\eta_D(p)p^i + g^{ij}(\mathbf{p})\eta^j(t), \quad (104)$$

with

$$\langle \eta^i(t)\eta^j(t') \rangle = \delta^{ij}\delta(t - t'). \quad (105)$$

Eq. (104) can be viewed as a particular case of the generic stochastic equation

$$\frac{dp^i}{dt} = f^i(\mathbf{p}) + g^{ij}(\mathbf{p})\eta^i(t). \quad (106)$$

One can then repeat the same steps followed in the one-dimensional case. From the Langevin equation one gets the expectation values:

$$\begin{aligned} \langle \Delta p^i \rangle &= f^i(\mathbf{p}_0)\Delta t + \alpha (\partial_k g^{ij}(\mathbf{p}_0)) g^{kj}(\mathbf{p}_0)\Delta t \\ \langle \Delta p^i \Delta p^j \rangle &= g^{ik}(\mathbf{p}_0)g^{jk}(\mathbf{p}_0)\Delta t = b^{ij}(\mathbf{p}_0)\Delta t, \end{aligned} \quad (107)$$

which lead to the Fokker-Planck equation:

$$\begin{aligned} \frac{\partial}{\partial t}P(\mathbf{p}, t) &= \frac{\partial}{\partial p^i} \left[-f^i(\mathbf{p}) - \alpha (\partial_k g^{ij}(\mathbf{p})) g^{kj}(\mathbf{p}) + \frac{1}{2} \frac{\partial}{\partial p^j} b^{ij}(\mathbf{p}) \right] P(\mathbf{p}, t) \\ &= \frac{\partial}{\partial p^i} \left[-f^i(\mathbf{p}) + \frac{1}{2} \partial_j (b^{ij}(\mathbf{p})) - \alpha (\partial_k g^{ij}(\mathbf{p})) g^{kj}(\mathbf{p}) + \frac{1}{2} b^{ij}(\mathbf{p}) \frac{\partial}{\partial p^j} \right] P(\mathbf{p}, t). \end{aligned} \quad (108)$$

Also in the d -dimensional case, requiring the Fokker-Planck equation to be independent on the discretization scheme and to admit a relativistic Maxwell distribution as a steady solution allows to fix the friction term entering into the Langevin equation and to relate it to the momentum-diffusion coefficients. One gets:

$$f^i(\mathbf{p}) = -\frac{1}{2T} b^{ij}(\mathbf{p}) \frac{\partial E_p}{\partial p^j} + \frac{1}{2} \frac{\partial b^{ij}(\mathbf{p})}{\partial p^j} - \alpha (\partial_k g^{ij}(\mathbf{p})) g^{kj}(\mathbf{p}), \quad (109)$$

which leads to

$$\begin{aligned} f^i(\mathbf{p}) &= -\frac{\kappa_L(p)}{2TE} p^i + \frac{1}{2} \left[\partial_p \kappa_L(p) + \frac{d-1}{p} (\kappa_L(p) - \kappa_T(p)) \right] \hat{p}^i \\ &\quad - \alpha \left[g_L(p) \partial_p g_L(p) + \frac{d-1}{p} g_T(p) (g_L(p) - g_T(p)) \right] \hat{p}^i. \end{aligned} \quad (110)$$

The friction coefficient to be employed in the Langevin equation can be then conveniently written (for the sake of simplicity we give it for the $\alpha = 0$ Ito discretization) as:

$$\eta_D^{\text{Ito}}(p) = \frac{\kappa_L(p)}{2TE} - \frac{1}{E^2} \left[(1-v^2) \frac{\partial \kappa_L(p)}{\partial v^2} + \frac{d-1}{2} \frac{\kappa_L(p) - \kappa_T(p)}{v^2} \right], \quad (111)$$

to be compared with the result given in Ref. [26]. The recipe employed to update the heavy-quark momentum is then the following:

$$\begin{aligned} p_{n+1}^i - p_n^i &= -\eta_D^{\text{Ito}}(p_n) p_n^i \Delta t + \xi^i(t_n) \Delta t \\ &\equiv -\eta_D^{\text{Ito}}(p_n) p_n^i \Delta t + g^{ij}(\mathbf{p}_n) \zeta^i(t_n) \sqrt{\Delta t}, \end{aligned} \quad (112)$$

with

$$\langle \zeta^i(t_n) \zeta^j(t_m) \rangle = \delta_{m,n} \delta^{i,j}. \quad (113)$$

Hence, at each time-step and for each quark, one has simply to extract d independent random numbers from a gaussian distribution with $\sigma = 1$, as it can be seen from Eq. (113).

C. Estimate of q_{\max}

In order to obtain a realistic estimate of q_{\max} to employ in the numerical calculations we adopt the following strategy. We take, as the upper bound of integration over the exchanged momenta, the ultraviolet cutoff given in Ref. [35]. The latter, in the limit $E_p \gg T$ required by our eikonal approach to be reliable, reads:

$$q_{\max} = \frac{2\langle k \rangle (E + p)}{\sqrt{M^2 + 2\langle k \rangle (E + p)}}. \quad (114)$$

In the above $\langle k \rangle \sim T$ represents an average momentum of the thermal particles taking part to the collisions. In Ref. [35] the authors let it vary from T to $3T$. In order to avoid plotting too many curves, our procedure is instead the following. We consider the non-relativistic limit (i.e. $M \gg T$) and we match the results for the momentum diffusion coefficient κ given by the QCD kinetic calculation [26]

$$3\kappa^{nr} = C_F \frac{g^4}{2\pi^3} \int_0^\infty k^2 dk \int_0^{2k} dq \frac{q^3}{(q^2 + m_D^2)^2} \times \left[\frac{N_f}{2} \frac{e^{\beta k}}{(e^{\beta k} + 1)^2} \left(2 - \frac{q^2}{2k^2} \right) + \frac{N_c}{2} \frac{e^{\beta k}}{(e^{\beta k} - 1)^2} \left(2 - \frac{q^2}{k^2} + \frac{q^4}{4k^4} \right) \right] \quad (115)$$

and by the HTL effective approach, namely

$$3\kappa^{nr} = C_F \frac{g^2 m_D^2 T}{2\pi} \int_0^{q_{\max}^{nr}} \frac{q^3 dq}{(q^2 + m_D^2)^2}, \quad (116)$$

where

$$m_D^2 = g^2 T^2 \left(\frac{N_c}{3} + \frac{N_f}{6} \right). \quad (117)$$

We found that, for the case of a coupling running with the temperature, the expression

$$q_{\max}^{nr} = 3.1Tg^{1/3}(T) \quad (118)$$

provides a good matching, with an agreement at the 1% level over the whole range of temperatures. Inserting the above expression into the zero momentum limit of Eq. (114) allows then to fix $\langle k \rangle$, and hence to determine the corresponding bound for general values of p .

References

- [1] T. Matsui and H. Satz, Phys. Lett. B 178 (1986) 416.
- [2] J. Adams *et al.* (STAR Collaboration), Phys. Rev. Lett. 92 (2004) 112301.
- [3] O. Barannikova, F. Wang *et al.* (STAR Collaboration), Nucl. Phys. A 715 (2003) 458c.
- [4] J. Adams *et al.* (STAR Collaboration), Phys. Rev. C 72 (2005) 014904.
- [5] K. Adcox *et al.* (PHENIX Collaboration), Phys. Rev. Lett. 89 (2002) 212301.
- [6] J. Adams *et al.* (STAR Collaboration), Phys. Rev. Lett. 91 (2003) 172302.
- [7] M. Shimomura (PHENIX Collaboration), Nucl. Phys. A 774 (2006) 457.
- [8] A. Adare *et al.* (PHENIX Collaboration), Phys. Rev. Lett. 98 (2007) 172301.
- [9] B.I. Abelev *et al.* (STAR Collaboration), Phys. Rev. Lett. 98 (2007) 192301.
- [10] H. van Hees, R. Rapp, Phys. Rev. C 71 (2005) 034907.

- [11] C.P. Herzog *et al.*, JHEP 0607 (2006) 013.
- [12] J. Casalderrey-Solana, D. Teaney, Phys. Rev. D 74 (2006) 085012.
- [13] J. Casalderrey-Solana, D. Teaney, JHEP 0704 (2007) 039.
- [14] S.S. Gubser, Nucl. Phys. B 790 (2008) 175.
- [15] H. Liu, K. Rajagopal, Y. Shi, JHEP 0808 (2008) 048.
- [16] W.A. Horowitz, M. Gyulassy, Phys. Lett. B 666 (2008) 320.
- [17] H. van Hees, M. Mannarelli, V. Greco, R. Rapp, Phys. Rev. Lett. 100 (2008) 192301.
- [18] P.B. Gossiaux, J. Aichelin, Phys. Rev. C 78 (2008) 014904.
- [19] P.B. Gossiaux, R. Bierkandt, J. Aichelin, arXiv:0901.0946 [hep-ph].
- [20] P.B. Gossiaux, J. Aichelin, arXiv:0901.2462 [nucl-th].
- [21] B. Alessandro *et al.* (ALICE Collaboration), J. Phys. G 32 (2006) 1295.
- [22] A. Beraudo, J.P. Blaizot, C. Ratti, Nucl. Phys. A 806 (2008) 312.
- [23] A. Beraudo, J.P. Blaizot, C. Ratti, arXiv: 0812.1130 [hep-ph].
- [24] T. Sjöstrand, P. Edén, C. Friberg, L. Lönnblad, G. Miu, S. Mrenna, E. Norrbin, Comp. Phys. Comm. 135 (2001) 238.
- [25] B. Svetitsky, Phys. Rev. D 37 (1988) 2484.
- [26] G.D. Moore, D. Teaney, Phys. Rev. C 71 (2005) 064904.
- [27] H. van Hees, V. Greco, R. Rapp, Phys. Rev. C 73 (2006) 034913.
- [28] R. Rapp, H. van Hees, arXiv: 0803.0901 [hep-ph].
- [29] Y. Akamatsu, T. Hatsuda, T. Hirano, arXiv: 0809.1499 [hep-ph].
- [30] C. Young, E. Shuryak, arXiv: 0803.2866 [nucl-th].
- [31] R.D. Pisarski, Phys. Rev. D 47 (1993) 5589.
- [32] F. Reif, Fundamentals of Statistical and Thermal Physics, McGraw-Hill, New York, 1965.
- [33] S. Caron-Huot, M. Laine, G.D. Moore, arXiv:0901.1195 [hep-lat].
- [34] Y. Koike, T. Matsui, Phys. Rev. D 45 (1992) 3237.
- [35] A. Adil, M. Gyulassy, W. Horowitz, S. Wicks, Phys. Rev C 75 (2007) 044906 (2007).
- [36] P. Chakraborty, M.G. Mustafa, M.H. Thoma, Phys. Rev. D 74 (2006) 094002.
- [37] J.P. Blaizot, E. Iancu, Phys. Rev. D 56 (1997) 7877.
- [38] A. Nakamura, T. Saito and S. Sakai, Phys. Rev. D 69 (2004) 014506.
- [39] E. Braaten, M.H. Thoma, Phys. Rev. D 44 (1991) 1298.
- [40] E. Braaten, M.H. Thoma, Phys. Rev. D 44 (1991) R2625.
- [41] R. Baier, Y.L. Dokshitzer, A.H. Mueller, S. Peigne, D. Schiff, Nucl. Phys. B 484 (1997) 265.
- [42] R. Baier, Y. Mehtar-Tani, arXiv: 0806.0954 [hep-ph].
- [43] M.C. Chu, T. Matsui, Phys. Rev. D 39 (1989) 1892.
- [44] O.Kaczmarek, F. Zantow, Phys. Rev. D 71 (2005) 114510.
- [45] S. Peigné, A. Peshier, Phys. Rev. D 77 (2008) 014015..
- [46] S. Peigné, A. Peshier, Phys. Rev. D 77 (2008) 114017.
- [47] M.L. Mangano, P. Nason, G. Ridolfi, Nucl. Phys. B 373 (1992) 295.
- [48] J.P. Blaizot, E. Iancu, Phys. Rept. 359 (2002) 355.
- [49] P. Kloeden, E. Platen, Numerical Solution of Stochastic Differential Equations, Springer, Heidelberg, 2000.
- [50] P. Arnold, Phys. Rev. E 61 (2000) 6091.
- [51] P. Arnold, Phys. Rev. E 61 (2000) 6099.
- [52] A.W.C. Lau, T.C. Lubensky, Phys. Rev. E 76 (2007) 011123.